Geodynamics of the Central Tethyan Belt revisited: Inferences from crustal magnetization in the Anatolia-Caucasus-Black Sea Region

V. Teknik [1]*, I. M. Artemieva [2,3,5]*, H. Thybo[1,4,5]

[1] Eurasia Institute of Earth Sciences, Istanbul Technical University, Istanbul, Turkey.

[2] Department of Geophysics, Stanford University, Stanford, CA, USA.

[3] Section of Marine Dynamics, GEOMAR Helmholtz Center for Ocean Research, Kiel, Germany.

[4] SinoProbe Laboratory, Chinese Academy of Geological Sciences, Beijing, China

[5] State Key Laboratory of Geological Processes and Mineral Resources, School of Earth Sciences, China University of Geosciences, Wuhan, China

*Corresponding authors: Vahid Teknik (vahid.teknik@gmail.com);

Irina Artemieva (iartemieva@geomar.de)

Key points:

- Magnetic regionalization does not fully match regional geological models in the Central Tethyan Belt.
- We identify previously unknown magmatic arcs and ocean relics.
- Magnetization is weak in Gondwana and strong in Laurentia terranes: Kirsehir massif has Laurentia affinity.

This article has been accepted for publication and undergone full peer review but has not been through the copyediting, typesetting, pagination and proofreading process, which may lead to differences between this version and the Version of Record. Please cite this article as doi: 10.1029/2022TC007282.

Abstract

We calculate the depth to magnetic basement and the average crustal magnetic susceptibility, which is sensitive to the presence of iron-rich minerals, to interpret the present structure and the tecto-magmatic evolution in the Central Tethyan belt. Our results demonstrate exceptional variability of crustal magnetization with smooth, small-amplitude anomalies in the Gondwana realm and short-wavelength high-amplitude variations in the Laurentia realm. Poor correlation between known ophiolites and magnetization anomalies indicates that Tethyan ophiolites are relatively poorly magnetized, which we explain by demagnetization during recent magmatism. We analyze regional magnetic characteristics for mapping previously unknown oceanic fragments and mafic intrusions, hidden beneath sedimentary sequences or overprinted by tectono-magmatic events. By the style of crustal magnetization, we distinguish three types of basins and demonstrate that many small-size basins host large volumes of magmatic rocks within or below the sedimentary cover. We map the width of magmatic arcs to estimate paleo-subduction dip angle and find no systematic variation between the Neo-Tethys and Paleo-Tethys subduction systems, while the Pontides magmatic arc has shallow (~15^{o}) dip in the east and steep (~50-55^{o}) dip in the west. We recognize an unknown, buried 450 km-long magmatic arc along the western margin of the Kırşehir massif formed above steep (55^{o}) subduction. We propose that lithosphere fragmentation associated with Neo-Tethys subduction systems may explain high-amplitude, high-gradient crustal magnetization in the Caucasus Large Igneous Province. Our results challenge conventional regional geological models, such as Neo-Tethyan subduction below the Greater Caucasus, and call for reevaluation of the regional paleotectonics.

Keywords

Crustal magnetization, magnetic basement, paleo-subduction, Tethyan Belt, magmatic arcs, sedimentary basins.

1. Introduction

The complex geodynamic evolution of Anatolia and the Caucasus region included the assembly of a mosaic of terranes of different tectonic origin during several pulses of collisional events associated with the closure of the Tethys oceans (Şengör and Yilmaz, 1981; Okay et al., 2001) and the Eurasia-Arabia collision. To date, evolutionary tectonic models for the region, largely based on geological and paleomagnetic data on outcrops of magmatic rocks and ophiolites (**Figure 1**), remain highly controversial (e.g. Ketin, 1966; Juteau, 1980; Şengör and Natal'in, 1996; Dilek et al., 1999; Stampfli, 2000; Bozkurt and Mittwede, 2001; Moix et al., 2008; Bozkurt, 2010; Robertson et al., 2013; Moghadam and Stern, 2015; Okay and Nikishin, 2015; Jolivet et al., 2016; Şengör et al., 2019). Geological field mapping cannot identify sutures and magmatic belts covered by sedimentary sequences or complicated by overprinted magmatic activity. The distribution of magmatic rocks buried within and below the sedimentary layer, and therefore unavailable for geological sampling, is crucial for understanding the regional paleotectonics, but is yet largely unknown.

Magnetic mapping provides an efficient tool for mapping hidden and buried magmatic structures and sutures (Blakely, 1995; Talwani and Kessinger, 2003; Lyngsie et al., 2006; Hinze et al., 2013). Here we use magnetic data, sensitive to the presence of iron-rich rocks at temperatures below the Curie point, to map at depth the distribution of unknown ophiolites and basaltic rocks associated with paleo-subduction systems and intraplate magmatism. Iron-

rich rocks of ophiolite complexes and magmatic arcs are usually highly magnetized (Hunt et al., 1995), thus allowing identification and determination of their subsurface extent by magnetic methods, such as was done for the Cascadia forearc (Blakely et al., 2005), the Mesozoic volcanic arc in the South China Sea (Li et al., 2018), mafic-ultramafic complexes below the Gobi Desert sediments (Ge et al., 2020), and the Oman ophiolite where geometry and offshore extent are unknown (Ali et al., 2020).

A strong magnetic susceptibility contrast between weakly magnetized sedimentary rocks and magnetized crystalline basement (Hunt et al., 1995) allows for calculating the depth to magnetic basement, which may be compared to the true basement depth determined from seismic or borehole data. In case the overlying sedimentary rocks do not include interbedded magnetic bodies (e.g. basaltic intrusions), the approach provides a proxy for the thickness of sedimentary sequences (Talwani and Kessinger, 2003) and is useful in regions with poor knowledge of the thickness of the sedimentary cover, such as in West Africa (Abdullahi et al., 2019) and Iran (Teknik and Ghods, 2017). The assumption that magnetic iron-rich bodies are absent within the sedimentary cover is not expected to be satisfied in most of Anatolia. In cases where the depths to magnetic and seismic basement disagree, certain conclusions can be made on the depth distributions of magnetized mafic and ultramafic rocks in the sedimentary cover and the upper crust. For example thick sedimentary sequences are identified both below and above a 3 km-thick layer of ~250 My old basalts of the Siberian traps (Cherepanova et al., 2013).

As our first result, we calculate the depth to magnetic basement, which we use for mapping the geometry and depth extent of sedimentary basins in Anatolia and surrounding regions. By comparing the depth to magnetic basement with seismic data on the depth to crystalline basement, we identify basins with interbedded magnetic bodies (mafic intrusions). As our second result, we calculate the average crustal magnetic susceptibility (magnetization)

and use this new regional magnetization model (i) to refine the geometry of geologically known magmatic arcs and ophiolites and (ii) to identify unknown, hidden and buried magmatic bodies. While magnetic data constrains the geodynamic origin of such magnetized bodies only indirectly through their geometry and depth extent, a comparison of magnetic models with other geophysical observations allows for testing geological interpretations against geophysical models. We apply this approach in our final result, where we propose a new model of tectono-magnetic regionalization.

Our study region in the west-central Tethyan Belt comprises, from west to east, the Aegean extensional region, the Central Anatolian microplates, the East Anatolian Plateau, the Lesser and Greater Caucasus, and the NW Iranian plateau. It also includes the SE Mediterranean Sea in the south and the Black Sea in the north. We start with a brief overview of major tectonic structures (**Section 2**) to provide an overview of basic geological information, important for our tectonic interpretations.

We next introduce basic concepts related to magnetic properties of lithospheric rocks (**Section 3**) and spectral analysis of magnetic data (**Section 4**). **Section 5** presents our magnetic modeling results, which we use for mapping magmatic arcs, ophiolite belts and sedimentary basins, some of them previously unknown. Finally, we discuss the results in relation to regional tectonics (**Section 6**) in order to refine geologically-based models of the tectono-magmatic evolution of Anatolia and surrounding regions. We conclude that some of the magnetic anomalies identified at depth: (i) indicate previously unknown large-scale structures, possibly related to yet unknown paleosubductions, (ii) some may rule out geologically-inferred subductions, (iii) some do not comply with local/regional geological models and do not follow tectonic features known from geological field mapping, (iv) some suggest different origin of sedimentary basins than inferred from exposed stratigraphic sequences, and (v) some question the Gondwana affinity of certain Anatolian blocks.

2. Geological setting

We summarize major tectonic and geodynamic features of the study region which had a very complex and debated tectonic evolution. This summary is intended to provide a general background for the discussion of our modeling results, and we intentionally omit some of the most disputed and controversial questions of its paleo-tectonics. These debates can be followed elsewhere (e.g. Şengör and Natal'in, 1996; Okay and Tüysüz, 1999; Stampfli, 2000; Moix et al., 2008; Bozkurt, 2010; Okay and Nikishin, 2015; Şengör et al., 2019).

2.1. Tethyan oceans, Eurasia and Gondwana terranes

The study region is part of the Alpine–Himalayan orogenic belt and includes Anatolia, Caucasus and the NW Iranian plateau as well as the adjacent Black Sea and NE Mediterranean Sea. Geological, paleomagnetic, and paleobiological data have been used to determine the affinities of different tectonic units of the region by their position with respect to the Eurasian plate (Laurasia), the Arabian plate (Gondwanaland), and the Tethyan oceans (Stampfli, 2000). The Eurasian (North Tethyan) units include the Scythian platform, the Greater and Lesser Caucasus, the Transcaucasus region between the two Caucasian ranges, the Pontides, and northern Anatolia north of approximately 40 °N (Şengör and Yilmaz, 1981). Other terranes of Anatolia, the southern Lesser Caucasus and Iran are probably of Gondwanan (South Tethyan) affinity (Stampfli et al., 2001; Adamia et al., 2011).

The Mesozoic closure of Paleo-Tethys led to the formation of arcs and back-arc structures at the southern margin of Eurasia, while the opening of Neo-Tethyan oceans provided a tectonic push from the south. Subsequent closure of the Neo-Tethys ocean, which began in the Jurassic, led to subduction-obduction of Neo-Tethys and accretion of a series of Gondwana-derived (Africa-Arabia) micro-plates to Eurasia (Khain, 1975; Şengör and Natal'in, 1996;

Stampfli, 2000; Bozkurt, 2010; Mosar et al., 2010; Hässig et al., 2013; Sosson et al., 2016) and, finally, ended with the Eurasia–Arabia continental collision. Several continental and oceanic fragments were assembled during the Late Cretaceous–Early Tertiary closure of the different branches of the Tethyan oceans (Zakariadze et al., 2007; Sosson et al., 2016).

This evolution is now marked by complex suture zones (Şengör and Yilmaz, 1981; Okay and Tüysüz, 1999; Moix et al., 2008; Şengör et al., 2019) (**Figure 1**) and a strongly heterogeneous structure of the crust and upper mantle (Piromallo and Morelli, 2003; Aydin et al., 2005; Mutlu and Karabulut, 2011; Salaun et al., 2012; Vanacore et al., 2013; Frederiksen et al., 2015; Topuz et al., 2017; McNab et al., 2018; Artemieva and Shulgin, 2019) with many controversial results. They are best explained by lithosphere thermo-compositional heterogeneity (Artemieva and Shulgin, 2019), such as associated with the Hellenic slab deformation, break-off and trench retreat in the west (Jolivet et al., 2012; Schildgen et al., 2014; McNab et al., 2018; Portner et al., 2018), fragmentation, tearing and detachment of Tethyan slabs in the north-east (Lei and Zhao, 2007; Zor, 2008; Eyuboglu, 2010; Govers and Fichtner, 2016), and lithosphere deformation in the Arabia-Eurasia collision zone in the south-east (Pearce et al., 1990; Turkoglu et al., 2008) and in the Caucasus region (Forte et al., 2014; Ismail-Zadeh et al., 2020).

2.2. Major terranes and tectonic units

Geologically, the region can be divided into a number of tectonic units and terranes **(Figure 1)** (Ketin, 1966; Şengör and Yilmaz, 1981; Görür et al., 1984; Okay and Tüysüz, 1999;Moix et al., 2008; Adamia et al., 2011; Sosson et al., 2016; Şengör et al., 2019). Below we briefly review the major ones from the north-east to the south and the west.

Greater and Lesser Caucasus

The Arabia-Eurasia continent-continent collision has led to the formation of the Greater and Lesser Caucasus orogens in the Mesozoic-Cenozoic with lithosphere deformation controlled by tectonic stresses from the northern edge of the Arabian plate at the Bitlis-Zagros suture. The age of the Tethyan closure and the onset of the collisional phase in the Greater Caucasus is highly debated and ranges from the Late Cretaceous to the Pliocene (cf. Adamia et al., 2011; Sosson et al., 2010, 2016; Forte et al., 2014; Cowgill et al., 2016; Ismail-Zadeh et al., 2020). Several phases of extension and compression are recognized during the opening and subsequent northward closure of various branches of the Tethyan oceans (e.g. Şengör and Natal'in, 1996; Rolland et al., 2010; Adamia et al., 2011; Okay and Nikishin, 2015; Sosson et al., 2016). The final closure of the oceans, leading to the collision between the Lesser Caucasus and the Scythian platform and the formation of the Greater Caucasus fold-and-thrust belt, is possibly as young as ca. 5 Ma (Leonov, 2007; Vincent et al., 2018; Cavazza et al., 2019). This collision also formed the Terek-Caspian flexural foreland basin (**Figure 1**) along the southern margin of the Scythian platform to the north of the Greater Caucasus.

Rioni-Kura Basins in the Transcaucasus region

Lithosphere deformation in the Caucasus region caused by the Eurasia-Arabia collision formed the Rioni-Kura sedimentary basins between the Greater and Lesser Caucasus mountain belts. These basins, connected to the Black Sea and South Caspian Sea basins, may have developed as foreland basins by flexural subsidence in the Tertiary as a response to orogenic processes in the Caucasus (Leonov, 2007; Mosar et al., 2010). The basins are very deep (10-20 km) (cf. Mangino and Preistley, 1998**,** Krasnopevtseva, 1984; Artemieva and Thybo, 2013) and are filled with Oligocene–Quaternary sediments from the Greater and the Lesser Caucasus (e.g. Ershov et al., 1999; Alizade and Khain, 2000; Brunet et al., 2003).

Black Sea basin

The Black Sea is often considered a back-arc basin formed in response to northward Neo-Tethys subduction in the Cretaceous Stephenson and Schellart, 2010). This process also led to the formation of the Pontides magmatic arc along the southern coast of the Black sea. The Black Sea consists of the Western and Eastern Black Sea Basins separated by the Mid-Black Sea High (the Andrusov Ridge) (**Figure 1**). Some studies suggest that the Eastern Black Sea may be a remnant of a Cretaceous oceanic basin (cf. Ismail-Zadeh et al., 2020), while strong lithosphere extension in the central Black Sea created a highly rifted continental crust in a coastal 100-200 km wide zone with possible presence of oceanic crust in the central parts of both the Western and Eastern Black Sea Basins (Nikishin et al., 2015b; Sosson et al., 2016). However, this interpretation remains speculative in the absence of crustal-scale seismic refraction data from the Western and Eastern Black Sea Basins.

Pontides

The Pontides fold-and-thrust belt along the present southern coast of the Black Sea includes the Western (Istanbul Terrane), Central and Eastern Pontides (**Figure 1b**). This orogenic system formed by southward dipping Paleo-Tethys subduction during Permo-Triassic time (e.g. Stampfli and Borel, 2002; Moix et al., 2008; Şengör et al., 2019) which also formed widespread accretionary complexes from the Marmara Sea to the Central Pontides. The Jurassic-Cretaceous arc volcanism and the presence of accreted rocks and forearc basins suggest the existence of a second subduction zone along the southern Pontides margin across the entire northern Anatolia (Topuz et al., 2014). During the Jurassic-Cretaceous, northward dipping subduction systems associated with closure of the Neo-Tethyan ocean created the Pontides volcanic arcs along the present southern coast of the Black Sea (Eyuboglu, 2010). During the late Mesozoic to middle Cenozoic these magmatic arcs were folded and thrusted toward the Black Sea (Okay and Nikishin, 2015).

Alborz mountains

The Pontides mountains continue in the east into the Lesser Caucasus and the Alborz orogenic belt south of the Caspian Sea (Moix et al., 2008; Şengör et al., 2019). Similar to the Pontides, the Alborz orogen in N Iran also experienced various collisional events related to the closure of the Tethyan oceans. During the late Paleozoic to early Mesozoic, the Central Iranian platform separated from Gondwanaland and collided with the Eurasian plate (Zanchi et al., 2009). However, the presence of Mesozoic–Cenozoic ophiolites of the Lake Van – Lake Urmia region near the Khoy-Van suture (**Figure 1b**) suggest that the Central Iranian platform was separated at that time from the North Anatolian platform by an ocean or a back-arc basin (Zonenshain and Pichon, 1986; Moghadam and Stern, 2015).

Zagros orogen and NW Iran

The Bitlis-Zagros suture marks the boundary between the Arabian Platform and Anatolia (Şengör and Yilmaz, 1981; Okay and Tüysüz, 1999). The Zagros fold-thrust orogenic system formed at the flank of the Arabian platform in the Late Cretaceous-Early Miocene as a result of the long-lasting Arabia-Eurasia convergence, which may have possibly included Neo-Tethys subduction/obduction followed by recent collisional processes (Moghadam and Stern, 2015; Teknik et al., 2019). In the east, the Main Zagros Thrust, marked by ophiolite fragments, separates the Zagros orogen from two magmatic arcs in NW Iran (the Sanandaj–Sirjan Zone in the west and the Urmia (Urumieh)-Dokhtar magmatic arc in the east) (**Figure 1b**). These arcs, trending parallel to the Zagros, formed by NE-ward Neo-Tethys subduction (Agard et al., 2011), and the Urmia-Dokhtar magmatic arc formed by the mid-Cenozoic collision of the Gondwana-derived Sanandaj-Sirjan Zone with the Eurasian continent (Hassanzadeh and Wernicke, 2016).

Central Anatolian Kırşehir massif (microplate)

The Kırşehir massif, a main tectonic unit of the Central Anatolian Plateau, is in parts surrounded by ophiolites (mostly in the north and south-east, **Figure 1b**). The massif drifted away from Gondwana during the Triassic (Şengör et al., 2019). Its collision with the Eurasian lithosphere at the Pontides was associated with northward subduction in the latest Cretaceous to Paleogene (Kaymakçi, 2000). The collision is marked by the approximately E-W trending Izmir-Ankara-Erzincan suture zone which runs across most of the northern Turkey (**Figure 1a**) (Şengör and Yilmaz, 1981).

Anatolides and Taurides

The Anatolides and Taurides form the fold-and-thrust belt along the southern margin of the Central Anatolian Plateau. These terranes separated from Gondwanaland in the Jurassic and were later accreted to the Pontides (Stampfli and Borel, 2002; Moix et al., 2008). The Anatolides-Taurides orogenic belt, formed by thrusting in Late Cretaceous to Eocene, hosts widespread Tethyan (~95–90 Ma) ophiolites, which originated in a possible intra-oceanic Neo-Tethys subduction zone (Gürer et al., 2016; Robertson et al., 2009). The evolution of the Anatolides may further have been affected by the debated Cyprus subduction (Kinnaird and Robertson, 2013).

Menderes Massif

The geodynamic evolution of western Anatolia, including the Menderes Massif, is dominated by distributed north-south extension marked by a series of subparallel graben structures. Lithosphere deformation is possibly associated with the active Hellenic subduction and probable slab rollback (Jolivet et al., 2013; Schildgen et al., 2014; Portner et al., 2018). The massif also hosts Late Precambrian gneisses, outcropping in the southern part (Robertson et al., 2013).

Sedimentary basins

Multiple series of subduction and continental convergence events formed different types of sedimentary basins in Anatolia since the Paleozoic (Robertson and Dixon, 1984; Şengör et al., 1984; Taymaz et al., 2007). Several sporadic, possibly interconnected, Late Cretaceous and the Eocene Anatolian basins with different dimensions can be categorized into fore-arc, intra-arc, and foreland basins. Remnants of Neo-Tethys oceanic crust may be preserved as ophiolites beneath the sedimentary cover of some of these basins (Görür et al., 1984, 1998; Rolland et al., 2010; Nairn et al., 2013; Gürer et al., 2016). However, in most of the Anatolian basins the structure and thickness of the sedimentary cover is still poorly constrained in the absence of conventional deep seismic reflection/refraction profiles. Notable exceptions are the Buyuk Menderes Graben in the west (Çifçi et al., 2011), the Çankırı Basin in the central part (Kaymakci ., 2000), and the Adana Basin in the south-east (Burton-Ferguson et al., 2005), but even in these basins depth conversion of seismic reflection profiles is uncertain in the absence of deep boreholes.

3. Magnetic anomalies

3.1. Sources of magnetic anomalies

Magnetic methods have notably contributed to our knowledge of the lithosphere structure. Medium- and short-wavelength anomalies in the magnetic field are caused by variations in the magnetization of rocks that are at temperatures below the Curie point. At long-wavelengths, magnetic signal of the lithosphere may overlap with the magnetic field from the core (Meyer et al., 1985; Maus, 2008), and such long-wavelength anomalies are of no importance for the present study. The magnetization of the lithosphere rocks is the sum of remanent and induced magnetization. The former exists only in ferromagnetic minerals (e.g. in magnetite

and titanomagnetite, minerals of major importance to crustal magnetism) and it is poorly constrained for the continental lithosphere. Therefore, practical modeling of magnetic data usually assumes that the continental magnetic field is dominated by induced magnetism caused by the present magnetic field of the Earth's core (Langel and Hinze, 1998; Fox Maule et al., 2005).

Induced magnetization depends primarily on (i) the magnetic susceptibility of rocks, (ii) the thickness of the magnetic layer, and (iii) the depth to its top (termed "depth to magnetic basement"). All three parameters are important for our analysis, and we briefly introduce them here.

3.2. Magnetic susceptibility

The magnetic susceptibility of rocks (measured in dimensionless SI units) is an intrinsic material property, which specifies the magnetic response of a rock to an external magnetic field. In particular, the average crustal magnetic susceptibility (ACMS, discussed in **Section 5.2**) is the ratio of induced rock magnetization (vertically averaged over the crustal column) to the intensity of the Earth's magnetic field. Depending on rock type, magnetic susceptibility varies across 4 orders of magnitude (**Figure 2b**) and its values are typically inversely correlated with the rock silica content (**Figure 2a**) (Clark and Emerson, 1991;Hunt et al., 1995). Besides, the magnetite content in rocks controls their magnetic susceptibility (**Figure 2b**) with the empirically determined rule: [*susceptibility*] ≈ *C* x [*volume fraction of magnetite*], with *C* between 2.5 (Shive et al., 1992) and 4.0, with an average C ~3.2 (Toft et al., 1990). Metamorphic reactions may also significantly change the magnetic susceptibility of rocks: in mantle peridotites magnetization increases with the degree of serpentinization (Oufi et al., 2002) (**Figure 2d**).

Igneous rocks have the largest magnetic susceptibility (0.10-0.20 SI) with the highest values measured in basalt, andesite, diabase, and peridotite. Susceptibility reduces to ca. 0.03-0.05 SI in felsic rocks and to near-zero values in most metamorphic and sedimentary rocks (Hunt et al., 1995) (**Figure 2a**). Due to the generally large contrast in magnetic susceptibility between sediments, granitic and metamorphic basement, and iron-rich mafic rocks, magnetic data provide an efficient tool for mapping sedimentary basins, buried magmatic arcs, igneous intrusions and ophiolite belts (which produce high average crustal magnetic susceptibility, see **Section 5.2**).

3.3. Curie depth point and thickness of the magnetic layer

Average crustal magnetization is proportional to the average crustal magnetic susceptibility (ACMS) and the thickness of the magnetic layer. The top of the magnetic layer is discussed below in **section 3.4**. The base of the magnetic layer is usually assumed to correspond to the Curie depth point, below which average magnetization tends to be zero. Thus the thickness of the magnetic layer is controlled by lithosphere composition and temperature, since the lithosphere geotherm defines the Curie depth point.

Rocks in the lithosphere have a broad range of Curie temperatures (strictly speaking, in ferrimagnetic material it is called the Néel temperature) which are controlled by composition, grain size and crystal structure of rock-forming minerals (Hunt et al., 1995). In titanomagnetites ($Fe_{3-x}Ti_xO_4$), which are the main magnetic minerals of igneous rocks, Curie temperature is strongly dependent on the amount and type of Fe- and Ti- oxides (**Figure 2c,** for detailed review of other factors see Jackson and Bowles, 2014). It increases almost linearly with decreasing proportion between Fe and Ti ($0<x<1$) and is 100-400 °C in most titanomagnetites and ca. 580 °C in magnetite (x=0), a common mineral in basaltic rocks (Hunt et al., 1995). In particular, ocean floor gabbros from a 1.2 Ma oceanic crust have Curie temperatures of 550-

600 ºC; but volcanics and dikes from the same area have Curie temperatures of 100-300 ºC due to differences in magnetic mineralogy (Varga et al., 2004). Differences in magnetic mineralogy also lead to significant variations in Curie temperatures of Variscan granites (Cruz et al., 2020) and rhyolites, andesites, and dacites from young volcanoes (Jackson and Bowles, 2014) (**Figure 2c**).

There is therefore a significant ambiguity in the choice of the critical temperature value representative of the lithospheric rocks, and the Curie temperature of 580 °C typical for magnetite is commonly adopted, because magnetite is the most abundant magnetic mineral in the crust, has the highest magnetization, and has the highest Curie temperature (Artemieva, 2011). In our discussion we adopt a Curie temperature of 580 °C for the Anatolian lithosphere; our choice is supported by an overall agreement between regional magnetic modeling of the Curie depth point (Aydin et al., 2005) and geothermal constraints on the depth to 580 °C isotherm, which ranges from 8-18 km in Western Anatolia to 20-32 km in Eastern Anatolia (Artemieva and Shulgin, 2019).

3.4. Depth to magnetic basement

The depth to magnetic basement (DMB, discussed in **Section 5.1**) refers to the top of the magnetic layer. DMB may be regarded as a proxy for the thickness of sedimentary rocks if the underlying basement has magnetic minerals (Talwani and Kessinger, 2003). The approach, important in regions without seismic or borehole data on the thickness of sedimentary cover, assumes that highly magnetized rocks lie immediately below the sedimentary cover that does not host iron-rich rocks (**Figure 3a**, cases 3-4). However, in many cases DMB may significantly differ from the depth to the true crystalline basement (termed hereafter “depth to seismic basement”, DSB) determined by drilling or seismic surveys. Below we compare the calculated DMB with seismic data on the depth to the crystalline basement to infer the

presence or absence of magmatic intrusions and ophiolites buried below sediments (**Section 5.1**).

In very deep (>10-15 km) basins with a hot lithospheric geotherm and a very shallow Curie depth point (CDP), the presence of iron-rich magmatic intrusions (basalts) within the upper part of a sedimentary sequence leads to shallower magnetic than seismic basement (**Figure 3a**, case 1). DMB can also be shallower than DSB if iron-rich rocks are all below the CDP and the sedimentary rocks are non-magnetic (i.e. DMB is close to zero, case 2). The opposite situation with magnetic basement deeper than seismic basement exists when the upper part of the crystalline crust does not contain magnetic sources, both in the case of a thick sedimentary basin (**Figure 3a,** case 5) and in the case when sedimentary cover is thin or absent (**Figure 3a**, case 6). DMB may also be deeper than DSB in regions with cold geotherm and CDP within the mafic lower crust (or below the Moho), so that lower crustal (and upper mantle) rocks preserve their magnetization (**Figure 3a**, case 7).

4. Method

4.1. Spectral analysis of magnetic data

The geodynamic evolution of Anatolia and adjacent regions is characterized by tectonic accretion of a series of Gondwana-derived and other terranes to Eurasia during closure of the Tethyan oceans, followed by neotectonic evolution in relation to the Eurasia-Arabia collision and dominated by lithosphere deformation by orogenesis associated with strike-slip faulting, wide-spread mafic magmatism, and extensional tectonics in the western domain, possibly related to slab roll-back around the Aegean Sea. We contribute to the analysis of the regional paleotectonic evolution by identifying outcropping and buried magmatic structures (basaltic

intrusions, magmatic arcs, oceanic fragments, ophiolites) and the geometry of known and unknown sedimentary basins by analyzing crustal magnetic susceptibility anomalies.

For the same rock magnetization, the magnitude and shape of magnetic anomalies depend on the depth (and geometry) of magnetized iron-rich bodies (**Figure 3b**): shallow magnetic bodies generally produce short-wavelength, high-amplitude magnetic anomalies, while deep bodies produce long-wavelength magnetic anomalies with smaller amplitude. The dependence of the wavelength of magnetic anomalies on the depth to the magnetic source forms the basis for a broad application of spectral techniques in analysis of the magnetic field, in particular for determining the depth to magnetic bodies, their geometry, and magnetization contrast. However, wide shallow magnetic bodies with smooth surface can also lead to long-wavelength anomalies, such that they will appear to originate from the deep crust. The analysis is described as "the most difficult in potential field inversion" (Blakely, 1995) because contributions from the bottom of magnetic bodies are, at all wavelengths, dominated by contributions from the top of these bodies, and therefore the bottom of magnetic bodies is hard to constrain (e.g. Spector and Grant, 1970; Blakely, 1988; Langel and Hinze, 1998).

Here we calculate two new regional magnetic models: the depth to magnetic basement (DMB) and vertically averaged crustal magnetic susceptibility (ACMS). We use a regional subset of a global Earth magnetic anomaly field EMAG2 (**Figure 4**), compiled from satellite, airborne and marine magnetic measurements (Maus et al., 2009; www.geomag.org/models/emag2.html). Over land, the resolution of the magnetic data is 1 arc-min at a height of 4 km above the geoid and is based on country-wide grids derived from airborne surveys. Offshore data sources include airborne and ship-track data with dense coverage in the Mediterranean and Black seas. The long-wavelength field was adjusted by the CHAMP satellite magnetic field (Maus et al., 2009; Khorhonen et al. (2007)). The overall nominal 2 arc-min

resolution of the magnetic data (i.e. 2-3 km lateral resolution) is well suited for crustal scale studies.

4.2. Calculation of depth to magnetic basement

To estimate the depth to magnetic basement (DMB) and vertically averaged crustal magnetic susceptibility (ACMS), we apply the radially averaged power spectrum method to the magnetic data. This method is widely used for estimating the Curie depth point (e.g. Blakely, 1988; Bouligand et al., 2009; Maus et al., 1997; Ross et al., 2006), and it was extended to calculating DMB and ACMS (e.g. Bouligand et al., 2009; Teknik et al., 2020; Teknik and Ghods, 2017). The solution is independent of a priori geological information.

The depth to magnetic basement is sensitive to the wavelength of the radially averaged power spectrum of the magnetic anomaly field (Maus et al., 1997; Teknik and Ghods, 2017; Zhou and Thybo, 1998). The spatial resolution is defined by the size of the averaging window and the overlap between adjacent windows (120 km × 120 km with 80% overlap between windows). This window size is based on the average wavelength of magnetic anomalies in typical basins of the region (**Figure 4a**). A smaller window size may not catch the whole wavelength of anomalies that contribute to the relief of magnetic basement, and a larger window size may mix the magnetic spectrum of adjacent anomalies. Sensitivity tests show that the lateral resolution of the DMB model is ca. 1/5 of the size of the averaging window (Teknik and Ghods, 2017), i.e. ca. 24 km in our regional DMB model. It means that local small-size magnetic anomalies are smoothed and their geometry may not be correctly resolved by the DMB model. Possible presence of non-vertical magnetic boundaries further may complicate interpretations (Gee and Kent, 2007). The uncertainty in the calculated depth to the top of the magnetic layer increases with depth, and for the chosen size of the averaging window it is less than 1 km if the top of the magnetic body is at a 5-10 km depth (Teknik and Ghods,

2017), allowing for high resolution of the DMB values in large-size magnetic anomalies. The choice of a smaller averaging window size increases the DMB uncertainty, which for a window size of 60 km × 60 km is ca. 3 km for a 10 km deep basin.

4.3. Calculation of crustal magnetization

ACMS represents the vertically averaged magnetic susceptibility from the surface to the Curie depth point, where temperature becomes sufficiently high to reduce the susceptibility of magnetized rocks to zero. ACMS depends on the amplitude of the radially averaged power spectrum curve (Teknik et al., 2020) and its spatial resolution is also defined by the averaging window size. The chosen window size is smaller than for DMB (60 km × 60 km with 80% overlap between adjacent windows), resulting in a lateral resolution of ca. 12 km for the ACMS model, which makes it possible to identify relatively short-wavelength magnetic anomalies from magmatic intrusions and ophiolites. Note that the calculated ACMS may not be representative of the true susceptibility if rocks have strong remanent magnetization (see **Section 3.1**).

Table 1. Abbreviations for Late Cretaceous to Paleogene basins and major magmatic arcs as labelled in Figures 4-8

AB	Adana Basin	VL	Van Lake Basin
B	Bijar Basin	CLIP	Caucasus Large Igneous Province
ÇB	Çankırı Basin	CSZ	Cyprus subduction zone
HB	Haymana Basin	TCFD	Terek Caspian foredeep
KB	Keban Basin	CPMA	Central Pontides magnetic anomaly
KrB	Kura Basin	DMA	Dardanelle magnetic anomaly
MB	Mianeh Basin	EPMA	Eastern Pontides magnetic anomaly

RB	Rioni Basin	NAMA	North Arabian/Cyprus magnetic anomaly
SB	Sivas Basin	NBMA	North Black Sea magnetic anomaly
TB	Tuzgölü Basin	NCMA	North Caucasus magnetic anomaly
ThB	Thrace Basin	UDMA	Urmia-Dokhtar magnetic anomaly
UB	Ulukışla Basin	WKMA	Western Kirşehir magnetic anomaly
UL	Urmia Lake Basin	WPMA	Western Pontides magnetic anomaly

5. Results: DMB and ACMS anomalies

5.1. Depth to magnetic basement (DMB)

How to interpret DMB anomalies?

A very heterogeneous pattern of DMB anomalies reflects a complex mosaic of crustal blocks of different tectonic origin, Paleo- and Neo-Tethyan sutures, paleo-subduction systems of various ages, ophiolite belts, and magmatic provinces. DMB anomalies show the depth to the top of magnetized bodies and may be interpreted in different scenarios, depending on the assumptions (see **Section 3** and **Figure 3** for explanations).

In the simplest interpretation, DMB provides a proxy for the total thickness of sedimentary sequence, assuming no magnetized rocks are present within the sediments. In this case, the overall regional pattern of the DMB distribution suggests that most of Anatolia has a thin sedimentary cover (typically 2-4 km) (**Figure 5a**). An alternative interpretation implies that a thick sedimentary cover of Anatolia includes a significant amount of magnetized basaltic rocks, associated with former wide-spread regional magmatic activity and presently covered by 2-4 km of sediments.

To discriminate between these two end-member options, we compare the depth to magnetic basement (DMB) with the depth to seismic (crystalline) basement (DSB) constrained by seismic and borehole data (**Figure 5b**). Note that DSB represents the true thickness of the sedimentary sequence (except for some ultra-deep basins with very high seismic velocity in the metamorphosed lower part of the basin), whereas DMB is not the true thickness, e.g. if magnetized rocks are present within the sedimentary sequence. In such cases DMB constrains the thickness of sediments above magnetized rocks (e.g. mafic intrusions, magmatic arcs, and ophiolite sequences at temperatures below the Curie point). Thickness of sediments is not well known from seismic studies for most of Anatolia and surrounding regions, in particular in western and central Anatolia where sparse data indicate a thin (<2 km) layer of sediments. Our compilation of sedimentary thickness (Artemieva and Shulgin, 2019) is based on the following data sources: the offshore domain is derived from the NOAA database (with unknown uncertainty of data) updated for the Black Sea where a high-resolution model of sedimentary thickness is based on a dense coverage of seismic reflection profiles (Nikishin et al., 2015a); the on-shore domain is derived from the EUNAseis seismic model based on a compilation of classical seismic refraction/reflection profiles (with, in general, sparse coverage in Anatolia; Artemieva and Thybo, 2013) and updated by other seismic studies for Turkey (Frederiksen et al., 2015; Gürbüz and Evans, 1991), compilation of various data for the Arabian plate (Stern and Johnson, 2010), and by borehole data for several Anatolian basins (cf. Görür et al., 1984; Nairn et al., 2013; Okay et al., 2001; Sosson et al., 2010).

With few exceptions, most of the Anatolian basins lack seismic studies of the crustal structure and thickness of sediments. In some basins (e.g. the Adana and the Çankırı basins), depth to the seismic basement is constrained by conventional seismic reflection sections, but with a highly uncertain depth conversion of seismic sections due to insufficient borehole information (Kaymakci ., 2000; Burton-Ferguson et al. 2005). For some basins, the depth to the

crystalline basement was derived from gravity data, which cannot provide unique constraints (Kaymakci ., 2000). Indirect constraints of sediment thickness based on exposed geological and stratigraphic sections, such as in the Ayhan-Büyükkışla basin where "all cross-sections are solely based on interpretations of the surface geology" (Advokaat et al., 2014, p. 1826) are unreliable for meaningful comparison with geophysical data. We do not include such speculative results to our DSB model due to their local character and usually unconstrained total depth to the crystalline basement.

Keeping in mind essential limitations of the DSB model, the results of comparison of the DMB and DSB models (i.e. the difference between the depth to the top of magnetized material and the seismically constrained depth to the crystalline basement) are presented in **Figure 6**. Various scenarios for tectonic interpretations are summarized in **Table 2**, and **Figure 3** provides further details.

Table 2. Comparison of depths to magnetic (DMB) and seismic basement (DSB)

	DSB > DMB	DSB = DMB	DSB < DMB
Physical explanation **(Figure 3)**	Magnetized magmatic (basaltic) material within sedimentary cover (at low temperature below the Curie point)	Sedimentary cover without magmatic material, underlain by magnetized basement rocks (e.g. magmatic rocks atop the basement, or felsic crust with minor iron-rich material at low temperature, or oceanic crust)	Sedimentary cover without magmatic material, underlain by basement rocks with low magnetization - either due to felsic, iron-poor composition or due to very high (close to the Curie point) crustal temperature. An end-member scenario includes a very thin sedimentary cover
Regional examples (**Figures 5b, 6a, 7a**).	• Volcanic province of S. Kirsehir massif; • Intra-orogenic basins (Rioni and Kura);	• Most orogens (the Pontides, E. Greater Caucasus, parts of the Taurides); • Volcanic provinces and high plateaux (E. Anatolia, Lesser Caucasus, NW Iran);	• Some orogens (the Anatolides, W. Greater Caucasus); • Massifs (Menderes, Rhodope, most of the Kırşehir massif);

	• Sanandaj-Sirjan Zone; Bitlis-Zagros and Khoy-Van suture zones; • Central deep basins of the Black Sea	• N. Arabian platform; • Parts of the Black Sea; Cyprus	• Small, often circular, basins of western-central Anatolia; • Terek-Caspian foredeep basin; • Some off-shore areas (E. Black Sea; NE Mediterranean)

Regions with small DMB

In on-shore regions, the smallest DMB (<3 km) is typical for orogens and high plateaux (NW Iran, the Pontides, Eastern Anatolia, the Lesser and the Greater Caucasus) (**Figure 5a**). A near-zero DMB anomaly at the Troodos ophiolite in Cyprus (**Figure 5a**) is caused by outcropping iron-rich rocks, which also cause a high crustal magnetic susceptibility (**Figure 7a**).

The Greater Caucasus is not associated with any clear magnetic anomaly, despite substantial volcano-magmatic activity of various ages in the collisional zone around Caucasus (Adamia et al., 2011), with predominantly calc-alkaline, subalkaline andesite-basalt, andesite-dacite rhyolite composition of the major post-collisional volcanoes of the Greater Caucasus (Tutberidze, 2004). Magnetic signature may also be expected for island arcs, back-arc basins, and intra-arc rifts accreted in the Greater Caucasus area with the closing of the Tethys Ocean. However, the Greater Caucasus has a shallow magnetic basement (about 2 km deep) which may reflect a thin sedimentary cover. We speculate that volcanic rocks of various ages may have lost their magnetization at high lithosphere temperature (Alexidze et al., 1993; Ershov et al., 2003), possibly associated with lithosphere delamination and the presence of hot asthenospheric material just below the crust (Koulakov et al., 2012). A small volume of magnetized rocks, as indicated by low average crustal susceptibility (**Figure 7a**) may be the

cause of near-zero DSB around the Elbrus stratovolcano, the highest mountain in the Caucasus and in Europe, dominated by dacites, andesites and rhyolites.

In the young volcanic provinces of Eastern Anatolia and along the southern boundary of the Kirsehir massif, small DMB <2 km (**Figure 5a**) is likely to indicate the presence of magnetized volcanic material within the sedimentary cover as illustrated by large positive values of [DSB-DMB] and very high crustal susceptibility (**Table 2, Figures 6a, 7a**). In contrast, the southern part of the Kırşehir massif with a linear belt of the Neogene mafic volcanoes and near-zero DMB (**Figure 5a**) does not show strong crustal magnetization. We explain this style by demagnetization at high crustal temperatures, as supported by the shallow depth to the Curie point (Aydin et al., 2005) (**Figure 6b**). This interpretation is consistent with seismic receiver function studies (Vinnik et al., 2014) and thermal modeling (Artemieva and Shulgin, 2019) which both indicate a 50–70 km thick lithosphere and therefore a high crustal temperature, which may explain the lack of magnetization of mafic rocks.

Transcaucasus

On-shore, the largest DMB (~8 km) is observed in the Kura foreland basin, where seismic data indicate the presence of a >15 km thick sedimentary sequence (Artemieva and Thybo, 2013) (**Figure 5b**). We interpret the inconsistency between the DMB and DSB values as an indicator for the presence of magnetized magmatic rocks within the lower portion of the sedimentary column. This interpretation is supported by the relatively strong crustal susceptibility in the Kura Basin (**Figure 7a**) which also suggests the presence of highly magnetized mafic volcanic rocks and/or ultramafic material (ophiolites) beneath or within the sedimentary cover. Our interpretation is consistent with regional geological data on intensive Late Jurassic, mainly basaltic, andesitic, dacitic and rhyolitic magmatism in the Kura Basin, followed by Late Cretaceous basalt-andesite and trachybasalt magmatism in the Kura Basin and parts of the Greater Caucasus (Lordkipanidze et al., 1989; Mederer et al., 2013). The

Saatli Superdeep Borehole drilled near the Kura River uncovered the thickest section of the island-arc volcanic series (dacites, andesites, basaltic andesites and basalts) at depths from 3540 m to the bottom of the borehole at 8324 m depth (Alizade and Khain, 2000), confirming our conclusions.

Basins of Central and Eastern Anatolian Plateau

DMB is around 5-6 km in most of the sedimentary basins in Central Anatolia (**Figure 5a**). These values are consistent with sediment thickness measurements in several boreholes (Nairn et al., 2013; Okay et al., 2001; Sosson et al., 2010), e.g. in the Tuzgölü basin where the DMB ~7 km is in agreement with a 6-7 km thick sedimentary sequence which includes turbiditic deposits, sandstones, siltstones, limestones, and no magmatic rocks (cf. Görür et al., 1984).

The Lake Van basin stands out as a DMB anomaly of ca. 4 km in a region with near-zero DMB values. The area includes chains of recent volcanoes and outcrops of post-collisional (with respect to the Late Cenozoic Eurasia-Arabia collision) magmatic rocks, responsible for very high crustal susceptibility (**Figure 7a**). Together with a large DMB, it indicates the presence of a significant volume of magnetized magmatic material in the sedimentary fill of the Lake Van basin (**Figure 6a**).

Black Sea

A dense coverage of the Black Sea by seismic reflection profiles (Nikishin et al., 2015b) allows comparison of the calculated depth to magnetic basement (**Figure 5a**) with depth to seismic basement (**Figure 5b**) which locally is deeper than 15 km. In the central part of the Eastern Black Sea, the DMB of 6-10 km is comparable to basement topography as interpreted from seismic data (5-10 km). Likewise, the seismic and magnetic models agree along the southern Black Sea coast and predict a basement depth of 4-6 km; in the western part of the

southern Black Sea DMB is smaller than DSB, but this region is at the edge of the resolved magnetic model.

The largest discrepancy between the seismic and magnetic depth to the basement occurs in the central deep basins of the Western and Eastern Black Sea, where the DMB is <6-8 km, while the seismic basement is at 10-17 km depth (**Figure 5ab**). We explain this discrepancy by the presence of magnetized basaltic rocks within the sedimentary column, possibly below the Miocene sequences as the DMB values suggest. This interpretation is in accord with interpretation of isometric highs on seismic reflection profiles in the Western Black Sea Basin as submarine (possibly Cretaceous) volcanic structures buried below the Eocene-Paleocene sedimentary sequence (Nikishin et al., 2015b). The transition from the on-shore to the off-shore regions, both in the Black Sea and NE Mediterranean, is generally marked by a sharp increase in DMB values from 3-5 km on-shore to 8-10 km off-shore.

Arabian plate and Scythian platform

Remarkably, a sharp step-like 3-5 km DMB deepening is observed along the northern edge of the Arabian plate and at the southern edge of the Scythian platform. Whereas the Anatolian DMB is shallow (typically <4 km), both the N Arabian plate and the S Scythian platform have DMB >6-10 km, locally exceeding 12 km (**Figure 5a**). The NE Arabian and Scythian plates, within our study region, do not have massive outcrops of magmatic rocks (**Figure 1b**) and therefore DMB is likely to constrain the true thickness of the nonmagnetic sedimentary cover. In the region of young volcanism in the NW part of the Arabian plate, the difference between the DSB and DMB values (with DSB being 1-4 km shallower than DMB) may be explained by the presence of weakly magnetized material below the thick sediments (**Figure 3a, case 5**), as also supported by low crustal susceptibility (**Figure 3b**).

In the southern part of the Scythian Platform, sparse seismic studies constrain the depth to the basement of ca. 6-8 km (Artemieva and Thybo, 2013) in general agreement with the DMB values of 6-10 km (**Figure 5a**). The anomaly centered around 44 ºN, 44 ºE with DSB>DMB (DMB ~6 km, **Figure 6a**) suggests the presence of weakly magnetized rocks in the lower portion of a >10 km thick sedimentary cover, if the sparse and old seismic data on the depth to the basement is correct. However, near-zero values of ACMS in this region question the reliability of old seismic interpretations (Neprochnov et al., 1975; Krasnopevtseva, 1984), so that the DMB values suggest that the sedimentary sequence is only ca. 6 km thick.

5.2. Average crustal magnetic susceptibility (ACMS)

Major features

We remind that crustal magnetization accounts only for the crustal column at temperatures below the Curie point (**Figure 6b**), and not necessarily down to the Moho. Average crustal magnetic susceptibility shows a complicated, patchy pattern of crustal magnetization with many short-wavelength anomalies (**Figure 7a**). High-amplitude short-wavelength ACMS anomalies require the presence of highly magnetized rocks at shallow depth (**Figure 3b**), while low-amplitude broad ACMS anomalies most likely are caused by deep magnetic bodies. Combined with the DMB model, average crustal magnetization allows to discriminate between various possible scenarios for the emplacement of mafic and ultramafic material into the shallow crust (**Figure 3a**).

Overall, low ACMS values are characteristic for regions south of ca. 40 °N, including the NE Mediterranean Sea, the Menderes Massif, the Taurides, the N Arabian plate, the Zagros orogen, and the Sanandaj-Sirjan zone in NW Iran. Most of this area has Gondwana affinity (originate from the South Tethyan) (Stampfli et al., 2001; Adamia et al., 2011).

Extremely low susceptibility in the tectonically active Menderes Massif cannot be explained by the primarily felsic composition of the igneous rocks, which are mostly basalts (Aldanmaz et al., 2006; Ersoy et al., 2010) (**Figure 7b**). Therefore, low crustal magnetization apparently reflects high crustal temperatures with the Curie depth locally expected at 10 km or less (Aydin et al., 2005; Artemieva and Shulgin, 2019) (**Figure 6b**). A local anomaly with high susceptibility in the Menderes Massif (38 ^{o}N, 28-29 ^{o}E, **Figure 7a**) is spatially related to known Precambrian basement rocks (Robertson et al., 2013), where the lithosphere is locally thickened to ca. 90 km (Artemieva and Shulgin, 2019) and crustal geotherms are sufficiently cold to preserve crustal magnetization.

The northern part of the study area (mostly within the Laurentia realm (Şengör and Yilmaz, 1981) has, in general, high susceptibility with short wavelength variations. This includes the Kirşehir massif, the Pontides, the Lesser Caucasus, the S margin of the Scythian platform, and the N and S Black Sea margins. The latter also have deep magnetic basement (**Figures 5a** and **7a**), and we interpret them as magmatic arcs along the Black Sea coasts which we discuss in the next section.

In contrast, the central part of the Black Sea (both the Eastern and Western Black Sea Basins) has low crustal magnetization, separated by a zone with high ACMS values approximately at around the Middle-Black Sea High (the Andrusov Ridge). This pattern does not mimic neither the depth to magnetic basement nor the seismically constrained sediment thickness (**Figure 5**), although a thick sedimentary cover clearly contributes to low ACSM values (**Figure 3b**).

Except for two well-known magmatic arcs (the Pontides in the north and the Urmia-Dokhtar in the east), most of the high susceptibility anomalies do not follow known tectonic structures. In particular, the strong Western Kirşehir Magnetic Anomaly, identified in this

study along the SW margin of the Kirşehir massif, has no correlation with any known magmatic outcrops (**Figure 7b**). However, as expected, many known magmatic outcrops are associated with high ACMS values.

Susceptibility gradient

To overcome problems with direct tectonic interpretation of the highly heterogeneous and complicated pattern of crustal magnetization anomalies, we calculate the gradient of the average crustal magnetic susceptibility (**Figure 8a**). A low susceptibility gradient is characteristic for regions with nearly uniform ACMS values, as in the southern part of the study area. In contrast, the Pontides and the Urmia-Dokhtar magmatic arcs, the Western Kirşehir Magnetic Anomaly, and the Caucasus Large Igneous Province have a strong susceptibility gradient and strong short-wavelength ACMS heterogeneity, which we interpret to be associated with voluminous basaltic magmatism in shallow bodies with rough shapes. Many sedimentary basins are also marked by high gradient anomalies. Importantly, some of the anomalies do not follow the known tectonic boundaries, such that the results provide new insights into regional geodynamic evolution.

6. Discussion: Regional pattern of magnetic anomalies

6.1. Styles of crustal magnetization

A major conclusion of our study is an extraordinary complexity of the regional pattern of crustal magnetization in Anatolia, especially in its central and eastern parts (**Figures 7a, 8a**). The results are in sharp contrast with a similar study for the Tethyan belt in Iran (Teknik et al., 2020), where a simple pattern of magnetic susceptibility variations is correlates with the

regional geology from surface observations, and therefore allows for straightforward tectonic interpretation.

To reduce the Anatolian susceptibility complexity to the level where tectonic interpretations are possible, we produced a simplified tectono-magmatic map (**Figure 8b, 8c**) which defines the main characteristic areas based on joint interpretation of susceptibility gradient (**Figure 8a**) and average crustal susceptibility (**Figure 7a**). Therefore, the map (which presents the main conclusion of our study) takes into consideration both the amplitude of magnetization anomalies and their spatial variation (**Table 3**).

Table 3. Major parameters controlling magnetic susceptibility and susceptibility gradient

Parameter	Amplitude of average magnetic susceptibility (**Figure 7a**)	Susceptibility gradient (**Figure 8a**)
Rock magnetic composition	Strong magnetization in iron-rich mafic and ultramafic rocks	Depends on amplitude variation and wavelength of rock magnetic susceptibility which is controlled by magnetic mineralogy
Temperature	Magnetization decreases to near-zero at high temperatures close to the Curie point	Depends on amplitude of rock magnetic susceptibility which is controlled by temperature
Depth to magnetized rocks	Shallow rocks produce anomalies with a stronger amplitude and with a shorter wavelength than deep rocks	Shallow rocks produce stronger gradient anomalies with a shorter wavelength than deep rocks

For basic information on the interpretation of magnetization anomalies we refer to **Section 3 and Figures 2 and 3**. Importantly, the magnitude of magnetic anomalies depends not only on the magnetic susceptibility of the rocks, but also on their depth: shallow magnetized bodies (intrusions) lead to stronger anomalies with shorter wavelengths than deep intrusions for the same rock magnetization (composition) (**Figures 3b, 9**). Temperature also affects susceptibility, such that the magnetization significantly decreases with temperature, and magmatic

rocks lose their magnetization when the temperature is close to the Curie point. A highly variable Curie temperature for rocks of different magnetic composition (**Figure 2c**) provides an additional complication for interpretation of ACMS and DMB in regions with high geothermal gradient and hot lithospheric geotherms, where rocks with magnetite as the major magnetic mineral may still preserve their magnetization, while rocks with a low-temperature Curie point may be demagnetized. Metamorphic reactions, such as serpentinization, and mineral alteration due to circulation of hydrothermal fluids also contribute to susceptibility variations (**Figure 2d**). We identify three major styles of the crustal magnetic susceptibility signal in the Anatolia-Caucasus region (**Figure 8b**):

H: regions with high-amplitude, short-wavelength variations in magnetic susceptibility. H-style is a characteristic of magmatic arcs and young magmatic provinces with a large volume of strongly magnetized rocks at shallow depths and at low temperatures.

M: regions with moderate susceptibility amplitude and relatively smooth regional variations. M-style indicates the presence of either deep highly magnetized rocks or shallow weakly magnetized rocks; the wavelength of magnetization anomalies helps to distinguish the two cases. M-style is observed primarily in the Kirsehir Massif and the Greater Caucasus.

L: low-intensity or non-magnetic regions with uniform, nearly-constant susceptibility values. L-style is typical for the Gondwana terranes in the western-southern Anatolia, Arabia, and the central Black Sea.

In the following section we discuss these magnetization styles in detail. Our results (**Figure 8b**) provide new structural information on major known tectonic units in the Anatolia-Caucasus region, and additionally we identify several hitherto unknown magnetization anomalies, which we associate with unknown sedimentary basins (**Figure 8c**), collisional structures

associated with the closure of the Tethys oceans, and pulses of magmatic activity in the region.

6.2. Deep basins (H- and L-magnetization)

Magnetic classification of deep basins

Many, but not all, Anatolian basins have strong crustal magnetization (H-style, pink colors in **Figure 8b;** Type 3, light green colors in **Figure 8c**), which is surprising because sedimentary basins are generally expected to have the lowest values of average crustal susceptibility (**Figure 2a)** and deep magnetic basement (DMB). This is, indeed, the case when no magmatic intrusions are present within the sedimentary cover (**Figure 3)**, and in such cases, DMB generally correlates with sedimentary thickness known from seismic models or drilling. However, in some Anatolian basins the DMB is shallower than the base of the sedimentary sequences (warm colors in **Figures 6a, c)**, suggesting the presence of iron-rich rocks within the sedimentary column (**Table 2**). In other locations, the DMB is deeper than the depth to the basement rocks (cold colors in **Figures 6a,c)** due to the presence of magnetized rocks with high susceptibility in the felsic upper crust, but not in the sediments (**Table 2, Figure 3a**).

We categorize deep basins into three types (**Table 4, Figure 8c**). Two of them have H-magnetization and one has L-magnetization style. Our categorization is based solely on magnetic susceptibility patterns and not on geological data, which may be potentially biased by limited exposed sections and outcrops, e.g. along roads and margins of basins.

Table 4. Types of deep basins by magnetic susceptibility patterns. See Figure 8c for locations.

	Type 1 basins	Type 2 basins	Type 3 basins
Typical tectonic setting	Basins in collisional orogens	Large platform basins and off-shore basins	Small, often circular, basins

Typical geodynamic mechanism	Lithosphere faulting and folding	Lithosphere flexure	Thermal relaxation
Examples	Basins of Transcaucasus and Caucasus region (Kura, Rioni, Terek-Caspian foredeep basin)	Basins of N Arabian plate and SW Scythian platform, Sivas Basin of C. Anatolia, Central Black Sea, NE Mediterranean Sea	Basins of C. Anatolia (Haymana, Tuzgölü, Keban, Adana), E. Anatolia (Van Lake), NW Iran (Bijar, Mianeh, Urmia Lake)
Depth to magnetic basement DMB (**Figure 5a**)	Deep (5-15 km)	Deep (5-15 km)	Moderate (4-8 km)
Geometry of susceptibility anomalies	Long (>200 km) linear belts	No specific shape, cover large areas	Small, circular
Average crustal magnetic susceptibility ACMS (**Figure 7**)	Very high (>0.05 SI)	Typically very low (<0.02 SI) with local highs (<0.05 SI)	Very high (>0.05 SI)
Susceptibility gradient (**Figure 8a**)	Very high, strong ACMS heterogeneity	Typically uniform ACMS values	Very high, strong ACMS heterogeneity
Magnetization style (**Figure 8b**)	H-magnetization	L-magnetization	H-magnetization
Proposed cause of magnetic susceptibility anomalies	Iron-rich rocks emplaced within a thick sedimentary cover along zones of paleo-collisions	Deep basins filled with non-magnetic rocks: either (1) sediments without mafic/ultramafic bodies, or (2) sediments with iron-rich bodies at temperatures above the Curie point	Iron-rich rocks emplaced locally within or below sedimentary cover in volcanic provinces (presently at temperatures below the Curie point)
Geological tectono-magmatic features	Often associated with known magmatic arcs and paleo-volcanoes	Typically not associated with known magmatic outcrops	Magmatic provinces with basaltic-type volcanism

Type I: Deep basins in collisional settings (H-magnetization)

The Kura Basin in the Transcaucasus has a very deep magnetic basement and extremely high average susceptibility (**Table 3, Figure 7**). This combination can be explained by the

presence of magmatic intrusions or trapped ophiolites below and within the lower parts of the >10 km thick sedimentary cover. These highly magnetized rocks are unknown in outcrops (**Figure 7b**), but in support of our interpretation a ca. 5 km thick sequence of magmatic rocks is uncovered below ca. 3.5 km depth in the Saatli Superdeep Borehole near the Kura River (Alizade and Khain, 2000).

Our results support a paleo-tectonic interpretation of the region in terms of northward-subduction (and obduction) of the Neo-Tethyan ocean which emplaced ophiolites and formed magmatic arc and back-arc structures at different times along the southern active Eurasian margin (e.g. Hässig et al., 2013; Şengör et al., 2019). However, the geometry and kinematics of the proposed, possibly several, subduction systems beneath the Kura Basin and the Eastern Pontides remain highly controversial (Avdeev and Niemi, 2011; Forte et al., 2014; Skolbeltsyn et al., 2014; Ismail-Zadeh et al., 2020) and we further discuss this in **Section 6.5** on the Greater Caucasus.

In contrast to the Kura Basin, the Rioni Basin has a notably weaker average susceptibility, although still high on average. The wavelength of strong small-scale heterogeneity can be explained by the presence of isolated, 50-100 km across, magmatic bodies within the sedimentary cover.

The Terek-Caspian Basin on the north-eastern side of the Greater Caucasus is traditionally interpreted as a foredeep basin (Ismail-Zadeh et al., 2020) associated with the Eurasia-Arabia collision. Our results suggest that the geodynamic mechanism of the basin subsidence may be more complicated, since a very high average crustal magnetic susceptibility (up to 0.20 SI) indicates the presence of, previously unknown, large volumes of a highly magnetized, iron-rich material in the basin fill (**Figure 7a**).

Type II: Large platform and ocean basins (L-magnetization)

The northern part of the Arabian plate and the SW Scythian platform have deep (6-12 km) magnetic basement (**Figure 5a**) with low average susceptibility (**Figure 7a**) suggesting that magmatic material and ophiolites are not dominant within and beneath the sedimentary cover. The thick sedimentary sequences in these large areas were deposited in non-magmatic environments associated e.g. with lithosphere flexure and/or extension in platform basins. Deep magnetic basement may also, in part, explain weak crustal magnetization (**Figure 9**), as an alternative to the lack of major mafic volcanism (the Arabian plate) and high crustal temperatures (the ocean domains).

Deep magnetic basement and low crustal magnetization are typical of the NE Mediterranean and Central Black Sea basins (blue colors in **Figure 8b**). The evolution of the NE Mediterranean Sea is consistent with thermal subsidence in oceanic basins, accompanied by voluminous marine sediment deposition enhanced by erosion of the adjacent continental regions. The Central Black Sea, where the presence of oceanic crust was proposed in some studies (e.g. Nikishin et al., 2015b), is clearly marked by a sharp decrease in the amplitude of average crustal susceptibility (**Figure 7a**) in sharp contrast with the magmatic arcs along the Black Sea coasts. We infer possible presence of oceanic crust in the West-Central (around 33 ^{o}E, 43 ^{o}N) and East-Central (around 37 ^{o}E, 43 ^{o}N) Black Sea by strong similarity between the style of magnetic susceptibility anomalies in these areas and the NE Mediterranean Sea basins.

The Sivas Basin at the SE margin of the Kirşehir Massif at the junction with the Pontides is the only Central Anatolian basin that belongs to type II (**Table 4**, blue colors in **Figure 8b**). The basin has low (<0.01 SI) average susceptibility (**Figure 7a**), and its shallow (~2 km) magnetic basement (**Figure 5a**) is similar to the known thickness of the sedimentary cover (**Figure 6a**). The geodynamic origin of the basin remains highly speculative, with geological

interpretations ranging from a remnant intra-oceanic basin (Yılmaz et al., 1997) to an extensional intracontinental (Dirik et al., 1999) or post-collisional foreland basin (Görür et al., 1998). These tectonic models do not suggest voluminous magmatic activity during basin evolution, in agreement with our results. We favor the same geodynamic interpretation for the origin of the Sivas Basin as for the basins in the N Arabian plate and the SW Scythian platform: sedimentation in non-magmatic environments caused by lithosphere deformation, possibly enhanced by the Arabia-Eurasia collision (Darin et al., 2018).

Type III: Small circular basins (H-magnetization)

We identify several isolated circular-shaped, high susceptibility anomalies (**Figure 7a**) which coincide with large DMB anomalies (**Figure 5a, Figure 10**), indicative of deep sedimentary basins (**Table 4**). Most of these basins are located away from the present plate boundaries (pink colors in **Figure 8bæ Type 3** light green colors in **Figure 8c**). In intraplate settings magma intrusion and its consequent cooling may create characteristic circular-shaped sedimentary basins (Kaminski and Jaupart, 2000) with high average magnetic susceptibility (**Figure 10**). A similar mechanism was also proposed as cause of a deep sedimentary basin above a series of large magmatic intrusions in the North Sea area (Sandrin and Thybo, 2008). By analogy with the latter model, we suggest that the subsidence of some of these isolated small Anatolian basins was caused by negative buoyancy from solidification and cooling of mafic intrusions in the crust. The thermal relaxation subsidence may, in places, be controlled by faults above a basement formed as an ophiolite mélange (Dirik et al., 1999).

Basins of Eastern Anatolia and NW Iran: Surprisingly, some of circular-shaped, high susceptibility basins with ca. 6 km depth to magnetic basement (e.g. the Van Lake, Keban, Bijar and Urmia Lake Basins) are located within the area of Miocene-Quaternary (in parts, still active) basaltic volcanism (**Figure 8b,c**). Preserved high crustal magnetization despite young volcanism, with magnetized rocks below 6 km depth, suggests that shallow (0-6 km deep)

magma chambers are present only locally around volcanoes, with major magma sources being deeper, below the Curie depth point at 15-20 km depth (**Figure 6b**). This conclusion is supported by relatively high Sn seismic velocities (Toksöz et al., 2008) and large lithosphere thermal thickness (ca. 100 km), which both suggest a cold regional geotherm with local thermal anomalies at the volcanic centers (Artemieva and Shulgin, 2019).

Given the recent magmatic activity, thermal subsidence or subsidence due to metamorphic reactions in the lower crust seem unlikely. Sufficient cooling of intrusions to produce basin subsidence probably cannot yet have taken place, unless basin subsidence was an isostatic response to past (>50 Ma) magmatic events (Bond and Kominz, 1991; Kaminski and Jaupart, 2000). In these basins, the subsidence may possibly originate from the presence of a thick high-density ophiolite layer beneath the sedimentary cover in paleo-forearc and intra-arc settings as proposed earlier for some Central Anatolian basins (e.g. Görür et al., 1998).

An alternative geological interpretation is based on the observation that the Van Lake, Keban, and Adana basins in S. Anatolia and the Bijar, Mianeh, and Urmia Lake basins in NW Iran form a chain located at almost constant distance of 100-120 km to the north and east of the Bitlis-Zagros suture zone. Geological inferences suggest that, at least some, of these basins may have formed in a forearc tectonic setting related to Neo-Tethys subduction (Robertson et al., 2013). However, typically forearcs have no magmatism, with the Izu-Bonin-Marianna forearc with boninitic iron-rich magmatic rocks being a notable exception (Macpherson and Hall, 2001). Our results indicate that these rounded basins are typically 100-200 km across with ca. 6 km deep magnetic basement, and they have high average crustal susceptibility, which requires the presence of highly magnetized rocks with the top at a ca 6 km depth. Therefore, our results do not support a forearc origin of these basins with a strongly magnetized crust.

Kirşehir massif (microplate) basins: Along the western and northern boundaries of the Kirşehir massif in central Anatolia, areas with deep magnetic basement (5-8 km) and an extremely high magnetization correlate with known basins, while outside these basins the depth to magnetic basement in the Kirşehir massif is 1-4 km. We interpret deep DMB combined with a high average susceptibility in the Kirşehir massif basins by the presence of a highly magnetic basement below a thick non-magnetic sedimentary sequence (**Figure 7a** and **Figure 10**). Borehole information in the Tuzgölü basin constrains a 6-7 km thick sequence of sedimentary rocks with no magmatic intrusions (cf. Görür et al., 1984; Sosson et al., 2010) which provides support to this interpretation. Our interpretation suggests the presence of a significant amount of basaltic intrusives in the crust which may have caused subsidence of the basins.

Our results only partially support geological inferences that many of these basins (including the Haymana, Tuzgölü and Çankiri basins) may have been a part of a larger basin system (Okay et al., 2001; Nairn et al., 2013)(**Figure 10**). The Haymana, Tuzgölü and Ulukışla Basins clearly appear to be associated with our newly identified Western Kirşehir magmatic arc (see next section) of a, yet unknown, subduction system with an unknown polarity. Since the basins are associated with strong magnetic anomalies, it is unlikely that they formed as forearc basins. Thus we argue that they may have formed as back-arc basins behind an eastward-dipping subduction beneath the Kirşehir microplate, given that they are located east of the Western Kirşehir magmatic arc **(Figure 11**). In this regard, these basins should be a part of a larger system of back-arc basins. However, the Çankırı Basin in the north-central Kirşehir massif clearly stands out as an isolated anomaly with a strong crustal magnetization, suggesting that the geodynamic evolution of the Çankırı Basin was different from the basins along the western flank of the Kirşehir massif **(Figure 11**).

6.3. Magmatic arcs (H-magnetization)

Dip angle of paleosubductions

Subduction systems are associated with (usually curved) magmatic arcs, formed by volcanism on the overriding plate and caused by magma generation primarily in the underlying mantle wedge. The composition of magmatic arcs reflects differences in composition of both the subducted material and the overriding plate (Pearce and Peate, 1995). These compositional differences lead to variations in magnetic mineralogy (**Figure 2**) and therefore should be reflected in patterns of crustal magnetization. In contrast to intermediate/felsic rocks typical of continental arcs, iron-rich basaltic/gabbroic rocks of oceanic arcs have high magnetic susceptibility. We therefore interpret long (>400-500 km), 50-200 km-wide belts with high magnetic susceptibility as (primarily) oceanic magmatic arcs associated with the closure of the Tethyan oceans (**Figure 7**). Zones of high susceptibility gradients, coinciding with zones of high susceptibility values, allow for recognizing contours of these magmatic arcs (pink colors in **Figure 8b**).

Known magmatic arcs associated with major collisional belts include the Pontides magmatic arc along the southern Black Sea coast, the East Anatolian magmatic arc associated with the Taurides, and the Urmia-Dokhtar magmatic arc in NW Iran associated with the Zagros orogen. Additionally, we recognize the previously unknown linear, ca. 450 km long, Western Kirşehir magmatic arc (WKMA in **Figure 8**) along the western margin of the Kirşehir massif. Notably, the Anatolides orogenic belt has no elongated magnetic anomaly which could be interpreted as a magnetic signature of a magmatic arc.

Subduction angle controls the arc width (Tatsumi and Eggins, 1995; Teknik et al., 2020) which commonly ranges between near-zero and 150-200 km. We use the width of the magmatic arcs identified by their magnetic susceptibility anomalies (**Figures 7, 8**) to estimate the

dip angle of paleosubduction (**Figure 12**). An interesting observation is a significant variability in the dip angle along the Pontides magmatic arc with a shallow (~15^{o}) dip in the east and a steep (~50-55^{o}) dip in the west. All other magmatic arcs fall within these bounds, with the largest subduction angle of ~55^{o} in the Urmia-Dokhtar, the Western Kirşehir, and the Cyprus magmatic arcs. There is no systematic variation in the dip angle between the Neo-Tethys and Paleo-Tethys subduction systems (**Figure 8b**).

Urmia-Dokhtar magmatic arc and East Anatolian Plateau

The Urmia-Dokhtar Magnetic Anomaly in NW Iran, parallel to the trend of the Zagros suture zone, marks the geologically well-studied Urmia-Dokhtar magmatic arc formed as a result of Neo-Tethys subduction (e.g. Agard et al., 2011). The distinct, strong magnetic anomaly of the magmatic arc appears to continue NW-ward towards the East Anatolian Plateau (**Figure 7a**) suggesting that the related subduction system may have continued into East Anatolia, where it may link to the North Black Sea Magnetic Anomaly or the Pontides anomaly. However, the magnetic anomalies sharply lose amplitude around the northern Lake Van Basin. Sharp termination of magnetic anomalies may be associated with crustal demagnetization in the area of active volcanism or it may mark a geological boundary, e.g. a branch of the Neo-Tethyan suture at the suggested Khoy-Van suture (Topuz et al., 2017) (ca. 38 ^{o}N, 46 ^{o}E in **Figure 8**). The latter interpretation is in line with geological studies of ophiolites of the Khoy-Van Lake region (around 37-39 ^{o}N, 44-45 ^{o}E) which suggest that an oceanic or back-arc basin separated the NW margin of the Iranian platform from the Anatolian platform in Mesozoic–Cenozoic time (Dercourt et al., 1986; Ismail-Zadeh et al., 2020).

Pontides and Black Sea margins

Our results indicate a highly variable dip angle of Paleo-Tethys subduction along the Pontides subduction system (**Figures 8b, 12n**). The high average susceptibility of the Pontides Magnetic Anomaly (**Figure 4, 7**) on- and off-shore along the whole southern Black Sea coast

largely follows the Central and Eastern Pontides orogenic belts (pink colors at PMA in **Figure 8b**). It is associated with magmatic arcs related to southward dipping Permo-Triassic Paleo-Tethys subduction (Okay and Tüysüz, 1999). This interpretation is supported by the presence of a chain of buried submarine Late Cretaceous volcanoes along the entire southern coast of the Black Sea (Nikishin et al., 2015b), in the area with high magnetic susceptibility.

A "mirrored" part of the Pontides Magnetic Anomaly is present off-shore along the northern coast of the Eastern Black Sea. The anomaly coincides with the Shatsky Ridge **(Figure 4b)** with a 30 km thick continental crust, which includes 4-8 km of sediments (Yegorova et al., 2020). The ridge is separated from the coast by a flexural basin (the Tuapse Trough) with a 10-15 km thick sedimentary sequence (Nikishin et al., 2015a). We therefore infer that a large volume of strongly magnetized, possibly mafic rocks underlies both the Shatsky Ridge and the Tuapse Trough, but in the latter the magnetic signature is weakened by a large depth to a magnetic body (see **Figure 3b**). A chain of buried Late Cretaceous (possibly Albian) volcanoes is known within a belt of high-amplitude, heterogeneous magnetic susceptibility off-shore the north-eastern coast of the Black Sea (NBMA in **Figure 8b**) (Nikishin et al., 2015b).

The North Black Sea Magnetic Anomaly is separated from the Pontides magmatic arc by a low susceptibility region in the Central Black Sea. We speculate that the North Black Sea and the Pontides Magnetic Anomalies may have been parts of the same magmatic arc, which separated in the Aptian-Cenomanian during rifting and back-arc basin extension that formed the Black Sea (Görür, 1988).

Northward extension of the Pontides Magnetic Anomaly indicates that the magmatic arc extends off-shore, in particular in its western part at the Istanbul Zone. At the western end of the Pontides, we identify the Dardanelle Magnetic Anomaly (DMA in **Figure 8b**) with patchy

high-amplitude susceptibility variations and 3-4 km deep magnetic basement. We interpret this magnetic anomaly by the presence of magmatic rocks within or below the sedimentary sequence. Tighter conclusions are not possible because the thickness of sediments is poorly constrained by seismic data. This magnetic anomaly may be associated with a Neo-Tethys subduction system with a highly curved subduction front and dip angle of ca. 30º (**Figure 12**).

Western Kirşehir Magnetic Anomaly

The eastern margin of the Anatolides includes a prominent magnetic feature: a linear, ca. 450 km long, 50-80 km wide belt with high crustal magnetization along the western margin of the Kirşehir massif, which we name the Western Kirşehir Magnetic Anomaly (WKMA in **Figure 8b**). Neither magmatic outcrops nor ophiolites have yet been mapped at the surface in this linear belt (**Figure 1b**). By analogy with other long linear magnetic anomalies, we interpret this, hithertoe unknown, susceptibility anomaly as a relic magmatic arc **(Figure 11)** formed above a steep subduction zone (ca. 55º, **Figure 12**) or trapped oceanic crust covered by sediments. Our results suggest an eastward extension of this anomaly below the Haymana and Tuzgölü Basins with an almost 6 km deep magnetic basement and very high average susceptibility (see discussion in **Section 6.2**).

Cyprus subduction and North Arabian magnetic anomaly

The debated Cyprus subduction system (e.g. Clube and Robertson, 1986; Morris, 1996) is marked by shallow DMB at the Troodos ophiolite (**Figure 5a**) and by a belt of increased average susceptibility which continues ca. 500 km eastward from Cyprus into the north Arabian plate approximately along 37 ºN latitude (**Figures 7a and 8b**). We name this high susceptibility belt, located ca. 100 km south of the Bitlis Suture along the southern edge of the western Zagros orogeny, the North Arabian Magnetic Anomaly (NAMA in **Figure 8b**). The anomaly, partially observed directly in magnetic data (**Figure 4**), has a patchy pattern of

magnetic susceptibility and is clearly marked by a high susceptibility gradient (**Figure 8a**). Its eastward extent into the north Arabian plate indicates that that the tectonic processes that formed Cyprus and the Troodos ophiolite may have extended far eastward over a larger zone than usually recognized and may have contributed to the geodynamic evolution of the north Arabian plate during the Eurasia-Arabia collision.

6.4. Caucasus Large Igneous Province (H-magnetization)

Strong magnetic anomalies with short-wavelength fluctuations and strong magnetization are present over large areas of the Eastern Caucasus, Transcaucasus, and the Lesser Caucasus. Their pattern is indicative of the presence of large volumes of highly magnetized material at shallow depths. We name the region between the Black and Caspian Seas with high-amplitude, high-gradient crustal magnetization the Caucasus Large Igneous Province (pink colors labelled CLIP in **Figure 8b**). Highly magnetized rocks may be associated with wide-spread Mesozoic, mainly basaltic and andesitic, magmatism in the Greater and Lesser Caucasus, in the Kura Basin of the Transcaucasus Massif and in NW Iran (Lordkipanidze et al., 1989; Mederer et al., 2013). Additionally, or alternatively, high crustal magnetization may be caused by the presence of oceanic fragments and Mesozoic back-arc domains, known from geological data (Hässig et al., 2013; Sosson et al., 2016). In particular, the presence of oceanic crust obducted over accreted Gondwana microplates of the Lesser Caucasus in the early Paleocene was inferred from geological data (Zonenshain and Pichon, 1986; Adamia et al., 2011; Okay and Nikishin, 2015; Sosson et al., 2016), and flat subduction of the back-arc basin between the Eurasia and Pontides arcs was proposed to explain the rapid post-Miocene uplift of the Greater Caucasus (Avdeev and Niemi, 2011).

There is an apparent contradiction between the presence of highly magnetized rocks (pink colors in **Figure 8b**) and young volcanism in the Caucasus LIP. Young LIPs imply hot crust

and demagnetization of the basaltic material at high temperatures. However, it is not the case in the Caucasus LIP. Thermal modeling indicates that the present-day lithosphere in this region is 125-150 km thick with only local thinning to 75-100 km (Artemieva and Shulgin, 2019). Regional P-wave (Bijwaard and Spakman, 2000; Piromallo and Morelli, 2003) and global S-wave tomography models (Shapiro and Ritzwoller, 2004; Schaeffer and Lebedev, 2013) also indicate that the lithosphere is ca. 150 km thick beneath the East Anatolian Plateau, the Caucasus, and NW Iran. These results are consistent with a 15-20 km deep Curie point (Aydin et al., 2005) (**Figure 6b**). The patchy, disrupted pattern of lithosphere thermal structure beneath the region may be caused by lithosphere fragmentation associated with Neo-Tethys subduction systems (Artemieva and Shulgin, 2019). It may favor an overall preservation of crustal magnetization due to a regionally cold lithosphere geotherm and only local crustal demagnetization in areas of young volcanoes. Emplacement of large volumes of magnetized magmatic material above lithosphere tear zones may explain the patchy, high-gradient pattern of crustal magnetization.

6.5. Moderately-magnetic regions (M-magnetization)

Greater Caucasus

The Greater Caucasus is characterized by medium-intensity, relatively homogeneous magnetization (green colors in **Figure 8b**). This magnetization style may be produced either by buried highly magnetized rocks, or by weakly magnetized shallow rocks, or by a combination of both. North-dipping Neo-Tethys subduction beneath the Greater Caucasus is commonly inferred from geological data (Zonenshain and Pichon, 1986; Guest et al., 2006; Mosar et al., 2010; Adamia et al., 2011; Sosson et al., 2016). In particular, the presence of a remnant northeast-dipping subduction at the northern edge of the Kura Basin and extending

beneath the Greater Caucasus has been proposed based on analysis of a deep earthquake below N Caucasus (Mellors et al., 2012). Neo-Tethys subduction models imply the presence of a magmatic arc with an associated belt of high-amplitude magnetization at around the Greater Caucasus.

We do not observe magnetic pattern typical of magmatic arcs along the strike of the Greater Caucasus and emphasize that neither gravity modeling (Kaban et al., 2018), nor the seismicity pattern support geodynamic models for subduction beneath the Greater Caucasus region. The only block with deep, localized, present-day seismicity in the area indicates that any subduction relic must be local and to the north of the Greater Caucasus at a very steep angle (Mumladze et al., 2015). We are also unaware of regional processes which may have caused demagnetization of the entire Greater Caucasus magmatic arc, if it existed. However, slightly higher crustal susceptibility in the western part of the Greater Caucasus (**Figure 7**), west of the Elbrus volcano and other main Cenozoic volcanoes, suggests that crustal magnetization in the eastern Greater Caucasus may have been weakened by Cenozoic and Mesozoic magmatism (Lordkipanidze et al., 1989; Mederer et al., 2013).

The presence of relatively shallow magnetic basement beneath the Greater Caucasus and the Alborz orogens with a nearly uniform depth of 1-3 km over a large area (**Figure 5a**) is also hard to reconcile with the geological interpretations that the Greater Caucasus may have formed by tectonic inversion of a Mesozoic continental back-arc basin formed behind Neo-Tethyan subduction (Zonenshain and Pichon, 1986; Mosar et al., 2010; Adamia et al., 2011; Avdeev and Niemi, 2011; Sosson et al., 2016). The Greater Caucasus and the Alborz orogens represent the northern edge of the deformation related to the Eurasia-Arabia collision against cold rigid lithosphere of the Scythian platform. We therefore suggest that shallow magnetic basement in the Greater Caucasus reflects folding and buckling of the crust (e.g. Cloetingh

and Burov, 2011), as also supported by the absence of any significant Bouguer gravity anomaly below the 3–5 km high elevation in the Greater Caucasus and the Alborz. Compressional buckling may have caused uplift of the Greater Caucasus and subsidence around them to create the deep basins, including the Rioni-Kura Basin.

Kirsehir massif and Taurides

The Kirsehir massif clearly stands out as an M-style magnetization block with a medium-to-high intensity of magnetic susceptibility with moderate heterogeneity (**Figures 8**), except for its strongly magnetic basins and flanking magmatic arcs (**Sections 6.2-6.3)**. Therefore, our results support geological interpretations that the massif may represent a separate microplate (Şengör and Yilmaz, 1981). However, crustal magnetization anomalies provide only partial support to geological models.

In classical interpretations, the Kirsehir massif is considered as part of Gondwanaland, from which it has drifted away during the Triassic (Stampfli, 2000; Şengör et al., 2019). However, our results show a sharp contrast in crustal magnetization of Laurentia and Gondwanaland terranes (high in the former and low in the latter, **Figure 8**). We therefore argue that magnetization may be an important discriminator between terranes of Laurentia and Gondwana origin, and thus by the pattern of crustal magnetization the Kirsehir massif is closer to Laurentian terranes.

The Taurides of southern Anatolia have, in general, low magnetic susceptibility (0.01-0.02 SI). Although Tethyan ophiolites are present there, they are not associated with high magnetization anomalies, possibly because of the proximity of Neogene volcanoes along the southern margin of the Kirsehir massif. Alternatively, low average crustal magnetic susceptibility may also suggest a small volume of basaltic additions to the crust.

Thrace Basin of western Anatolia

The triangular-shaped Cenozoic Thrace basin to the north of the Marmara Sea and west of the Istanbul Zone has a 5-7 km deep magnetic basement and low crustal susceptibility. We interpret this pattern by the absence of magmatic intrusions both within the thick sedimentary cover and, possibly, within the upper crust. Therefore, our interpretation supports geological conclusions on a forearc origin of the basin, which may have formed over metamorphic basement. However, low crustal susceptibility does not support the presence of a wide-spread ophiolite mélange in the southern part of the basin (Keskin, 1974; Siyako and Huvaz, 2007; Elmas, 2012).

6.6. Non-magnetic regions (L-magnetization)

Large non-magnetic basins of the northern Arabian platform and the ocean domains with low and uniform susceptibility are discussed in **Section 6.2**. Identification of regions with low magnetic susceptibility (blue colors in **Figure 8b**) is as important for understanding the paleotectonic evolution, as identification of magmatic arcs and deep basins with high magnetization. The absence of strong magnetic susceptibility anomalies implies:

(i) absence (or minor volume) of basaltic magmatism, whereas felsic magmatism (such as associated with continental arcs) cannot be ruled out;

(ii) absence (or minor volume) of oceanic material (including ophiolites) at shallow depth,

(iii) a very hot crust, close to the Curie temperature, which may cause demagnetization of iron-rich basaltic rocks, if present.

Menderes Massif of Western Anatolia

The Menderes Massif in western Anatolia stands out as an anomalous area with near-zero average crustal magnetic susceptibility (**Figure 7a**), and with a depth to magnetic basement

remarkably larger (>4 km) than in eastern Anatolia (typically <2 km) (**Figure 5a**). Regional evolution, essentially controlled by the Hellenic subduction with possible slab rollback (Jolivet et al., 2013), is dominated by strong lithosphere extension, rifting and widespread Late Miocene to Pleistocene basaltic volcanism. Iron-rich basaltic rocks should be highly magnetized at low temperatures.

We explain near-zero crustal magnetization in western Anatolia by high geothermal gradient, where high temperatures close to the Curie point have essentially demagnetized any magmatic rocks. Our conclusion is supported by a very shallow Curie depth in the Menderes Massif (Aydin et al., 2005) (**Figure 6b**). The rifted part of the western Menderes Massif has some of the highest measured heat flux values in Anatolia (>100 mW/m^2) and an anomalously hot lithosphere, possibly thinned to the Moho (Artemieva and Shulgin, 2019).

Similarly, the belt of Tethyan ophiolites along the SE edge of the Menderes Massif (**Figure 1**) is not marked by a strong magnetization anomaly as one would expect for iron-rich oceanic fragments. This observation also requires very high present-day crustal temperatures, in agreement with both thermal modeling and Curie depth estimates (Aydin et al., 2005; Artemieva and Shulgin, 2019). The near-zero magnetic anomalies in most of the Anatolides also suggest either the presence of non-magnetic basement or high temperature (Artemieva, 2019; Artemieva and Shulgin, 2019) which reduces magnetic susceptibility and the thickness of the magnetized crustal crust.

Zagros orogen and Sanandaj-Sirjan zone

The Gondwana terranes of southern Anatolia and NW Iran typically have low crustal magnetization. Despite a significantly different tectonic evolution, the Zagros fold-and-thrust belt and the Sanandaj-Sirjan zone NE of the Bitlis-Zagros suture share similar patterns of magnetic anomalies. The average crustal magnetization is very small and locally almost zero,

except for a few locations with high susceptibility anomalies (**Figure 4 and 7a**). The magnetic basement is shallow (typically 0-4 km) in both regions, in contrast to the Arabian plate where it is deep (10 km and more), while average crustal magnetization is also very small. Both the Zagros fold-and-thrust belt and the Sanandaj-Sirjan zone have, in general, thick and cold lithosphere (Artemieva and Shulgin, 2019), so that thermal demagnetization is unlikely. Thus low crustal magnetization suggests that mafic magmatism, if any, played only a minor role in the geodynamic evolution. Likewise, our results do not indicate the presence of trapped oceanic material in Zagros and the Sanandaj-Sirjan zone, such as associated with Mesozoic or Cenozoic oceanic subduction. We therefore favor the interpretation that the Zagros fold-and-thrust belt formed as an accretionary orogen.

7. Summary and Conclusions

We contribute to the analysis of the regional paleotectonic evolution of the Central Tethyan Belt by calculating the depth to magnetic basement and average magnetic susceptibility of the crust by the radially averaged power spectrum method. We combine these two new magnetic models with the calculated gradient of crustal magnetization to map tectonic structures with different amplitudes, wavelengths and depths of origin of crustal magnetization anomalies. We also constrain the size and depth of major sedimentary basins in the region, and present a review of tectonic interpretations of crustal magnetic models. Our results identify three styles of crustal magnetization typical of specific geodynamic settings, which we discuss in relation to lithosphere thermo-chemical structure and tectono-magmatic processes.

Interpretation of the new magnetic results, together with regional geological data on magmatism and ophiolites and with regional geophysical data on the lithosphere thermal structure, confirms known and constrains new tectono-magmatic features of the region. We summarize

our results in a new tectono-magnetic map (cf. **Figure 8b,c**) and make the following conclusions.

- **Magnetic regionalization does not fully match regional geological models:**

  Poor correlation between known ophiolites and magnetization anomalies indicates a small volume of presently magnetized material in the Tethyan ophiolites, which we explain by demagnetization during recent magmatism. There is no direct correlation between the crustal magnetization anomalies and known major tectonic boundaries, many constrained by ophiolitic belts. Exceptions are the Kirşehir massif boundaries and the central Paleo-Tethys suture, which roughly follows the southern edge of the Pontides Magnetic Anomaly. The major seismogenic zones (the North Anatolian and Eastern Anatolian strike-slip faults) are not reflected in the magnetic susceptibility anomalies.

- **Gondwana and Laurentia terranes have different magnetization styles:**

  Crustal magnetization may be an important discriminator between terranes of Gondwana and Laurentia. The amalgamated terranes of Gondwana affinity in Southern Anatolia, the northern Arabian plate, and the Zagros exhibit very low and uniform crustal magnetization. The transition to the terranes with Laurasia affinity in north-central Anatolia at ca. 40 ^{o}N latitude is marked by a notable increase in amplitude of magnetization and an appearance of short-wavelength magnetization heterogeneity, indicative of the presence of large amounts of mafic magmatic bodies at shallow depth. By the pattern of crustal magnetization, the Kirsehir massif is similar to Laurentia terranes, and not to Gondwana terranes as inferred in earlier geological interpretations.

- **Neo-Tethyan and Paleo-Tethyan magmatic arcs are associated with a broad range of subduction dip angles:**

High-amplitude, high-gradient magnetization anomalies mark known magmatic arcs (the Urmia-Dokhtar in NW Iran, the Pontides in N Anatolia) associated with Tethyan subduction systems. The geometry of magnetization anomalies around the Black Sea coast suggests that the original magmatic arc may have split by rifting of the Central Black Sea into two parts, now located along the southern (the Pontides) and northern coasts of the Black Sea (the previously unknown North Black Sea magmatic arc). The debated Cyprus subduction system, with the pattern of crustal magnetization similar to magmatic arcs, extends ca. 500 km eastwards of Cyprus into the N. Arabian plate, suggesting that its tectonic extent has been underestimated, and that the associated tectonic processes may have been important in the Arabia/Eurasia collision.

The dip angle of paleosubduction systems (between ~15^{o} and ~55^{o}) estimated from the inverse correlation between arcs width and slab dip shows no systematic variation between the Neo-Tethys and Paleo-Tethys subduction systems. A significant variability in the dip angle exists along the strike of the Pontides magmatic arc with a shallow (~15^{o}) dip in the east and a steep (~50-55^{o}) dip in the west.

- **Hitherto unknown ~450 km long, Western Kirşehir magmatic arc is buried under 6 km of sediments:**

The very strong, ca. 450 km long, magnetic anomaly along the western margin of the Kirşehir massif is not associated with outcrops of magmatic or ophiolitic rocks. It marks the presence of a hitherto unknown relic magmatic arc or trapped oceanic relic buried below a ca. 6 km thick sedimentary strata. We interpret the anomaly as a relic magmatic arc formed above a steep (ca. 55^{o}) subduction **(Figure 11)**.

- **Greater Caucasus and Zagros are not associated with Tethyan subduction:**

The Greater Caucasus does not have magnetization anomalies typical of magmatic arcs and, therefore, our results do not support geological inferences on north-dipping Neo-Tethys subduction below the Greater Caucasus. Instead we propose that compressional folding and buckling of the crust related to the Eurasia-Arabia collision may explain shallow magnetic basement and medium-intensity, relatively homogeneous magnetization in the Greater Caucasus region. Likewise, low, uniform crustal magnetization and cold lithospheric geotherms in the Zagros fold-and-thrust belt are explained by its formation as an accretionary orogen.

- **Lesser Caucasus hosts the Caucasus Large Igneous Province:**

We identify the Caucasus LIP by high-amplitude, high-gradient crustal magnetization associated with wide-spread Mesozoic magmatism, which may be caused by lithosphere fragmentation in Neo-Tethys subduction systems. High crustal magnetization preserved in areas of young volcanoes indicates regionally cold lithosphere geotherms with only local crustal demagnetization responsible for high-gradient short-wavelength magnetization anomalies.

- **Superdeep basins of the Caucasus region host magnetized iron-rich rocks within or below a thick sedimentary cover:**

The Transcaucasus Kura-Rioni basins and the Terek-Caspian foredeep basin have high crustal magnetization despite a very deep (5-15 km) magnetic basement. We explain their magnetic style by the presence of highly magnetized mafic volcanics and/or ultramafic material (ophiolites) beneath or within the lower part of their thick sedimentary cover. A strong magnetization anomaly north-east of the Greater Caucuses questions a purely flexural origin of the Terek-Caspian basin subsidence and suggests that thermo-chemical buoyancy was an important factor in its evolution.

- **Small isolated basins of Central Anatolia and NW Iran all host strongly magnetized rocks within sedimentary cover:**

We explain the origin of several isolated, 100-200 km wide, circular-shaped sedimentary basins (Haymana, Tuzgölü, Çankırı, Keban, Adana, Van Lake, Bijar, Mianeh, Urmia Lake) by subsidence due to negative buoyancy from solidification and cooling of large mafic intrusions in the crust or the presence of oceanic relics, as supported by high crustal magnetization and 4-8 km deep magnetic basement. The Haymana, Tuzgölü and Ulukışla basins of the Kirşehir massif may have formed as back-arc basins behind eastward-dipping subduction marked by the hitherto unknown Western Kirşehir magmatic arc. We explain the preservation of strong crustal magnetization in the Van Lake, Keban and Urmia Lake Basins located within the area of young (in parts, still active) basaltic volcanism by deeply-seated major magma chambers (below the Curie depth point), with only narrow feeding channels below the volcanoes.

- **Crust of Western Anatolia is demagnetized by high temperature:**

Exceptionally low susceptibility in the Menderes Massif, in a region of widespread basaltic magmatism, is consistent with extremely high crustal temperature, which lead to the loss of rock magnetization.

- **Platform basins of the Arabian and Scythian plates have non-magnetic thick sedimentary sequences:**

Basins of the N Arabian and SW Scythian stable platforms have very low average crustal magnetization and very deep (5-15 km) magnetic basement. This combination indicates a very minor role of intra-sedimentary magmatic material in the basin subsidence.

- **West-Central and East-Central Black Sea basins may have oceanic crust:**

Weak, uniform crustal magnetization in the NE Mediterranean Basin is representative of oceanic crust covered by very thick (ca. 10 km) sedimentary sequences. From strong similarity between the style of magnetic susceptibility anomalies in the NE Mediterranean and the

Black Sea basins we infer the possible presence of oceanic crust in the West-Central (ca. 33 ^{o}E, 43 ^{o}N) and East-Central (ca. 37 ^{o}E, 43 ^{o}N) Black Sea. We also infer the presence of magnetized basaltic rocks within the Black Sea sedimentary cover, possibly below the Miocene sequences at 6-8 km depth.

- **Our results challenge many aspects of conventional regional geological models:**

Our results are only partially consistent with tectonic models for the Central Tethyan belt, largely derived from geological mapping of exposed ophiolites and outcropping magmatic rocks. We demonstrate that a large volume of magmatic bodies associated with relic magmatic arcs and trapped oceanic fragments is buried under several kilometers of sediments. Our results challenge many aspects of conventional regional geological models and call for reevaluation of the regional paleotectonic evolution.

Acknowledgments

HT and IA acknowledge grant #92055210 from the National Science Foundation of China. VT is financed by ITU BAP (Turkey) grant #42338 to HT and by Large Grants from the Danish Research Council FNU16-059776-15 to IMA and DFF-1323-00053 to HT. The authors enjoyed many discussions with A.M.C. Şengör, B.A. Natal'in, A.I. Okay, and other collegues at ITU on the tectonics of Anatolia. Two anonymous reviewers are acknowledged for identifying parts of the text that required further clarification for general readership.

Data Availability Statement:

Magnetic data is available at http://www.geomag.org/models/emag2.html and for permanent archive at http://earthref.org/cgi-bin/er.cgi?s=erda.cgi?n=970

References

Abdullahi, M., Kumar, R., Singh, U. K., 2019. Magnetic basement depth from high-resolution aeromagnetic data of parts of lower and middle Benue Trough (Nigeria) using scaling spectral method. J. African Earth Sci., 150, 337-345,

Adamia, S., Zakariadze, G., Chkhotua, et al., 2011. Geology of the Caucasus: A review. Turkish J. Earth Sci. 20, 489–544. https://doi.org/10.3906/yer-1005-11

Advokaat, E.L., van Hinsbergen, D.J.J., Kaymakcı, N. et al., 2014. Late Cretaceous extension and Palaeogene rotation-related contraction in Central Anatolia recorded in the Ayhan-Büyükkışla basin. Intern. Geology Review, 56, 1813–1836. http://dx.doi.org/10.1080/00206814.2014.954279

Agard, P., Omrani, J., Jolivet, L., et al., 2011. Zagros orogeny: a subduction-dominated process. Geol. Mag. 148, 692–725. https://doi.org/10.1017/S001675681100046X

Aldanmaz, E., Köprübaşi, N., Gürer, Ö.F., et al., 2006. Geochemical constraints on the Cenozoic, OIB-type alkaline volcanic rocks of NW Turkey: Implications for mantle sources and melting processes. Lithos 86, 50–76. https://doi.org/10.1016/ j.lithos.2005.04.003

Alexidze, M.A., Gugunava, G.E., Kiria, D.K., Chelidze, T.L., 1993. A three-dimensional stationary model of the thermal and thermoelastic fields of the Caucasus. Tectonophysics 227, 191–203. https://doi.org/10.1016/0040-1951(93)90094-Z

Ali, M.Y., Watts, A.B., Searle, M.P. et al., 2020. Geophysical imaging of ophiolite structure in the United Arab Emirates. Nature Commun. 11: 2671. https://doi.org/10.1038/s41467-020-16521-0

Alizade, A., Khain, V. E. (Eds.), 2000. The Saatly Superdeep Borehole (SG–1). Nafta-Press, Baku, 211 pp. (in Russian).

Amante, C., Eakins, B.W., 2009. ETOPO1 1 Arc-Minute Global Relief Model: Procedures, Data Sources and Analysis, NOAA Technical Memorandum NESDIS NGDC-24. https://doi.org/10.1594/PANGAEA.769615

Artemieva, I.M., 2011. The Lithosphere: An Interdisciplinary Approach. Cambridge University Press, 794 pp. https://doi.org/10.1017/CBO9780511975417

Artemieva, I.M., 2019. Lithosphere structure in Europe from thermal isostasy. Earth-Science Rev. 188, 454–468. https://doi.org/10.1016/j.earscirev.2018.11.004

Artemieva, I.M., Shulgin, A., 2019. Geodynamics of Anatolia: Lithosphere Thermal Structure and Thickness. Tectonics 38, 4465–4487. https://doi.org/10.1029/2019TC005594

Artemieva, I.M., Thybo, H., 2013. EUNAseis: A seismic model for Moho and crustal structure in Europe, Greenland, and the North Atlantic region. Tectonophysics 609, 97–153. https://doi.org/10.1016/j.tecto.2013.08.004

Avdeev, B., Niemi, N.A., 2011. Rapid Pliocene exhumation of the central Greater Caucasus constrained by low-temperature thermochronometry. Tectonics 30, 2. https://doi.org/10.1029/2010TC002808.

Aydin, I., Karat, H.I., Koçak, A., 2005. Curie-point depth map of Turkey. Geophys. J. Int. 162, 633–640. https://doi.org/10.1111/j.1365-246X.2005.02617.x

Bijwaard, H., Spakman, W., 2000. Non-linear global P-wave tomography by iterated linearized inversion. Geophys. J. Int. 141, 71–82. https://doi.org/10.1046/j.1365-246X.2000.00053.x

Blakely, R.J., 1988. Curie temperature isotherm analysis and tectonic implications of aeromagnetic data from Nevada. J. Geophys. Res. 93, 11817. https://doi.org/10.1029/jb093ib10p11817

Blakely, R.J., 1995. Potential theory in gravity and magnetic application, Cambridge University Press, New York, NY

Blakely, R.J., Brocher, T. M., Wells, R. E., 2005. Subduction zone magnetic anomalies and implications for hydrated forearc mantle. Geol. Soc of Amer. Bull., 33, 445-448.

Bond, G.C., Kominz, M.A., 1991. Disentangling Middle Paleozoic sea level and tectonic events in cratonic margins and cratonic basins of North America. J. Geophys. Res. 96, 6619–6639. https://doi.org/10.1029/90JB01432

Bouligand, C., Glen, J.M.G., Blakely, R.J., 2009. Mapping Curie temperature depth in the western United States with a fractal model for crustal magnetization. J. Geophys. Res. Solid Earth 114, 1–25. https://doi.org/10.1029/2009JB006494

Bozkurt, E., 2010. Neotectonics of Turkey – A synthesis. Geodinamica acta 14, 3-30

Bozkurt, E., Mittwede, S.K., 2001. Introduction of the geology of Turkey – A synthesis. International Geology Review 43 (7), 578–594

Brunet, F.F., Korotaev, M. V., Ershov, A. V., Nikishin, A.M., 2003. The South Caspian Basin: A review of its evolution from subsidence modelling. Sediment. Geol. 156, 119–148. https://doi.org/10.1016/S0037-0738(02)00285-3

Burton-Ferguson, R., Aksu, A.E., Calon, T.J., Hall, J., 2005. Seismic stratigraphy and structural evolution of the Adana Basin, Eastern Mediterranean. Mar. Geol. 221, 153–183. doi:10.1016/j.margeo. 2005.03.009

Cavazza, W., Albino, I., Galoyan, G., Zattin, M., Cattò, S., 2019. Continental accretion and incremental deformation in the thermochronologic evolution of the Lesser Caucasus. Geosci. Front. 10, 2189–2202. https://doi.org/10.1016/j.gsf.2019.02.007

Cherepanova, Y., Artemieva, I.M., Thybo, H., Chemia, Z., 2013. Crustal structure of the Siberian craton and the West Siberian basin: An appraisal of existing seismic data. Tectonophysics 609, 154–183. https://doi.org/10.1016/j.tecto.2013.05.004

Çifçi, G., Pamukçu, O., Çoruh, C., et al., 2011. Shallow and deep structure of a supradetachment basin based on geological, conventional deep seismic reflection sections and gravity data in the Buyuk Menderes Graben, western Anatolia. Surveys in Geophysics, 32, 271–290. doi:10.1007/s10712-010-9109-8

Clark, D.A., Emerson, D.W., 1991. Notes on rock magnetization characteristics in applied geophysical studies. Explor. Geophys. 22, 547–555. https://doi.org/10.1071/EG991547

Cloetingh, S., Burov, E., 2011. Lithospheric folding and sedimentary basin evolution: A review and analysis of formation mechanisms. Basin Res. 23, 257–290. https://doi.org/10.1111/j.1365-2117.2010.00490.x

Clube, T.M.M., Robertson, A.H.F., 1986. The palaeorotation of the troodos microplate, cyprus, in the late mesozoic-early cenozoic plate tectonic framework of the Eastern Mediterranean. Surv. Geophys. 8, 375–437. https://doi.org/10.1007/BF01903949

Cruz, C., Sant'ovaia, H., Noronha, F., 2020. Magnetic mineralogy of Variscan granites from northern Portugal: an approach to their petrogenesis and metallogenic potential. Geologica Acta, 18.5, 1-20. DOI: 10.1344/GeologicaActa2020.18.5

Darin M.H., Umhoefer P.J., Thomson S.N., 2018. Rapid Late Eocene Exhumation of the Sivas Basin (Central Anatolia) Driven by Initial Arabia-Eurasia Collision. Tectonics, doi: 10.1029/2017TC004954

Dercourt, J., Zonenshain, L.P., Ricou, L.-E., et al., 1986. Geological evolution of the tethys belt from the atlantic to the pamirs since the LIAS. Tectonophysics 123, 241–315. https://doi.org/10.1016/0040-1951(86)90199-X

Dilek,Y., Thy, P., Hacker,B., Grundvig, S., 1999. Structure and petrology of Tauride ophiolites and mafic intrusions (Turkey): implications for the Neotethyan Ocean. Geological Society of America Bulletin 111 (8), 1192–1216.

Dirik, K., Göncüoğlu, M.C., Kozlu, H., 1999. Stratigraphy and pre-Miocene tectonic evolution of the southwestern part of the Sivas Basin, Central Anatolia, Turkey. Geol. J. 34, 303–319. https://doi.org/10.1002/(SICI)1099-1034(199907/09)34:3<303::AID-GJ829>3.0.CO;2-Z

Elmas, A., 2012. The Thrace Basin: stratigraphic and tectonic-palaeogeographic evolution of the Palaeogene formations of northwest Turkey. Int. Geol. Rev. 54, 1419–1442. https://doi.org/10.1080/00206814.2011.644732

Ershov, A. V., Brunet, M.-F., Korotaev, M. V., et al., 1999. Late Cenozoic burial history and dynamics of the Northern Caucasus molasse basin: implications for foreland basin modelling. Tectonophysics 313, 219–241. https://doi.org/10.1016/S0040-1951(99)00197-3

Ershov, A. V., Brunet, M.F., Nikishin, A.M., et al., 2003. Northern Caucasus basin: Thermal history and synthesis of subsidence models. Sediment. Geol. 156, 95–118. https://doi.org/10.1016/S0037-0738(02)00284-1

Ersoy, E.Y., Helvac, C., Palmer, M.R., 2010. Mantle source characteristics and melting models for the early-middle Miocene mafic volcanism in Western Anatolia: Implications for enrichment processes of mantle lithosphere and origin of K-rich volcanism in post-collisional settings. J. Volcanol. Geotherm. Res. 198, 112–128. https://doi.org/10.1016/ j.jvolgeores.2010.08.014

Eyuboglu, Y., 2010. Late Cretaceous high-K volcanism in the eastern Pontides orogenic belt: Implications for the geodynamic evolution of NE Turkey. International Geology Review, 52, 142-186.

Forte, A.M., Cowgill, E., Whipple, K.X., 2014. Transition from a singly vergent to doubly vergent wedge in a young orogen: The Greater Caucasus. Tectonics 33, 2077–2101. https://doi.org/10.1002/2014TC003651

Fox Maule C., Purucker, M., Olsen, N., Mosegaard, K., 2005. Heat flux anomalies in Antarctica revealed by satellite magnetic data. Science, 309, 464–467.

Frederiksen, A.W., Thompson, D.A., Rost, S., et al., 2015. Crustal thickness variations and isostatic disequilibrium across the North Anatolian Fault, western Turkey. Geophys. Res. Lett. 42, 751–757. https://doi.org/10.1002/ 2014GL062401

Ge, T., Qiu, L., He, J., et al., 2020. Aeromagnetic identification and modeling of mafic-ultramafic complexes in the Huangshan-Turaergen Ni-Cu metallogenic belt in NW China: Magmatic and metallogenic implications. Ore Geology Reviews, 127, 103849, https://doi.org/10.1016/j.oregeorev.2020.103849.

Gee, J.S., Kent, D.V., 2007. Source of oceanic magnetic anomalies and the geomagnetic polarity timescale. In: Treatise on Geophysics, v. 5, Elsevier, 419-458.

Görür, N., 1988. Timing of opening of the Black Sea basin. Tectonophysics 147, 247–262. https://doi.org/10.1016/0040-1951(88)90189-8

Görür, N., Oktay, F.Y., Seymen, İ., Şengör, A.M.C., 1984. Palaeotectonic evolution of the Tuzgölü basin complex, Central Turkey: sedimentary record of a Neo-Tethyan closure. Geol. Soc. London, Spec. Publ. 17, 467–482. https://doi.org/10.1144/GSL.SP. 1984.017.01.34

Görür, N., Tüysüz, O., Şengör, A.M.C., 1998. Tectonic evolution of the Central Anatolian basins. Int. Geol. Rev. 40, 831–850. https://doi.org/10.1080/ 00206819809465241

Govers, R., Fichtner, A. 2016. Signature of slab fragmentation beneath Anatolia from full-waveform tomography. Earth and Planetary Science Letters, 450, 10–19

Guest, B., Axen, G.J., Lam, P.S., Hassanzadeh, J., 2006. Late Cenozoic shortening in the west-central Alborz Mountains, northern Iran, by combined conjugate strike-slip and thin-skinned deformation. Geosphere 2, 35. https://doi.org/10.1130/ges00019.1

Gürbüz, C., Evans, J.R., 1991. A seismic refraction study of the western Tuz Gölü basin, central Turkey. Geophys. J. Int. 106, 239–251. https://doi.org/10.1111/j.1365-246X.1991.tb04614.x

Gürer, D., van Hinsbergen, D.J.J., Matenco, L., Corfu, F., Cascella, A., 2016. Kinematics of a former oceanic plate of the Neotethys revealed by deformation in the Ulukışla basin (Turkey). Tectonics 35, 2385–2416. https://doi.org/10.1002/2016TC004206

Hassanzadeh, J., Wernicke, B.P., 2016. The Neotethyan Sanandaj-Sirjan zone of Iran as an archetype for passive margin-arc transitions. Tectonics 35, 586–621. https://doi.org/ 10.1002/2015TC003926.

Hässig, M., Rolland, Y., Sosson, M., et al., 2013. Linking the NE Anatolian and Lesser Caucasus ophiolites: Evidence for large-scale obduction of oceanic crust and implications for the formation of the Lesser Caucasus-Pontides Arc. Geodin. Acta 26, 311–330. https://doi.org/10.1080/09853111.2013.877236

Hinze, W.J., von Frese, R.R. B., Saad, A.H., 2013. Gravity and Magnetic Exploration: Principles, Practices, and Applications. Cambridge University Press, 522 pp.

https://doi.org/10.1016/j.jafrearsci.2018.11.006.

Hunt, C.P., Moskowitz, B.M., Banerjee, S.K., 1995. Rock Physics & Phase Relations: A Handbook of Physical Constants. AGU Ref. Shelf 3, 189–204. https://doi.org/ 10.1029/RF003

Ismail-Zadeh, A., Adamia, S., Chabukiani, A., et al., 2020. Geodynamics, seismicity, and seismic hazards of the Caucasus. Earth-Science Rev. https://doi.org/10.1016/j.earscirev.2020.103222

Jackson, M., Bowles, J. A. 2014. Curie temperatures of titanomagnetite in ignimbrites: Effects of emplacement temperatures, cooling rates, exsolution, and cation ordering, Geochem. Geophys. Geosyst., 15, 4343– 4368, doi:10.1002/2014GC005527.

Jolivet, L., Faccenna, C., Agard, P., et al., 2016. Neo-Tethys geodynamics and mantle convection: from extension to compression in Africa and a conceptual model for obduction. Canadian Journal of Earth Sciences, 53(11): 1190-1204.

Jolivet, L., Faccenna, C., Huet, B., et al. 2012. Aegean tectonics: Strain localisation, slab tearing and trench retreat. Tectonophysics, 597-598, 1–33. https://doi.org/10.1016/j.tecto.2012.06.011

Jolivet, L., Faccenna, C., Huet, B., et al., 2013. Aegean tectonics: Strain localisation, slab tearing and trench retreat. Tectonophysics 597–598, 1–33. https://doi.org/10.1016/j.tecto.2012.06.011

Juteau, T., 1980. Ophiolites of Turkey. Ofioliti 2, 199–238.

Kaban, M.K., Petrunin, A.G., El Khrepy, S., Al-Arifi, N., 2018. Diverse Continental Subduction Scenarios Along the Arabia-Eurasia Collision Zone. Geophys. Res. Lett. 45, 6898–6906. https://doi.org/10.1029/2018GL078074

Kaminski, E., Jaupart, C., 2000. Lithosphere structure beneath the Phanerozoic intracratonic basins of North America. Earth Planet. Sci. Lett. 178, 139–149. https://doi.org/10.1016/S0012-821X(00)00067-4

Kaviani, A., Paul, A., Moradi, A., and et al., Crustal and uppermost mantle shear wave velocity structure beneath the Middle East from surface wave tomography, Geophysical Journal International, Volume 221, Issue 2, May 2020, Pages 1349–1365, https://doi.org/10.1093/gji/ggaa075

Kaymakçi, N., 2000. Tectono-stratigraphical evolution of the Çankırı Basin (Central Anatolia, Turkey). Geol. Ultraiectina. N190.

Keskin, C., 1974. The stratigraphy of the northern Ergene Basin., in: 2nd Petroleum Congress of Turkey, Ankara. 137–163.

Ketin, I., 1966. Tectonic units of Anatolia (Asia Minor). Bulletin of the Mineral Research and Exploration Institute of Turkey 66, 23–34.

Ketin, İ., 1966. Tectonic units of Anatolia. Maden Tetk. ve Aram. Bull. 66, 23–34.

Khain, V.E., 1975. Structure and main stages in the tectono-magmatic development of the Caucasus: an attempt at geodynamic interpretation. Am. J. Sci. 275–A, 131–156.

Khorhonen, J.K., Fairhead, J.D., Hamoudi, M., Hemant, K., Lesur, V., Mandea, M., Maus, S., Purucker, M.E., Ravat, D., Sazonova, T., ThØbault, E., Magnetic Anomaly Map of the World—Carte des Anomalies Mag-nétiques du Monde. Scale: 1:50,000,000, 1st edn. (Commission for the Geological Map of the World,2007)

Kinnaird, T., Robertson, A. 2013. Tectonic and sedimentary response to subduction and incipient continental collision in southern Cyprus, easternmost Mediterranean region. Geological Society London Sp. Publ., 372, 585-614. https://doi.org/10.1144/SP372.10.

Koulakov, I., Zabelina, I., Amanatashvili, I., Meskhia V., 2012. Nature of orogenesis and volcanism in the Caucasus region based on results of regional tomography. Solid Earth, 3, 327–337, https://doi.org/10.5194/se-3-327-2012

Krasnopevtseva, U. V., 1984. Deep structure of the Caucaus seismoactive region. Nauka, Moscow, 109 pp. (in Russian).

Langel, R.A., Hinze, W.J., 1998. The magnetic field of the Earth's lithosphere: the satellite perspective. Cambridge University Press, 448 pp., https://doi.org/10.1017/ CBO9780511629549

Lei, J., Zhao, D. 2007. Teleseismic evidence for a break-off subducting slab under eastern Turkey. Earth and Planetary Science Letters, 257, 14–28.

Leonov, Yu. G. (Ed.), 2007. The Greater Caucasus in the Alpine Epoch. GEOS, Moscow, 368 pp. (in Russian).

Li, F., Sun, Z., Yang, H., 2018. Possible spatial distribution of the Mesozoic volcanic arc in the present-day South China Sea continental margin and its tectonic implications. J. Geophys. Res., 123, 6215–6235. https://doi.org/10.1029/ 2017JB014861

Lordkipanidze, M.B., Meliksetian, B., Djarbashian, R., 1989. Mesozoic–Cenozoic magmatic evolution of the Pontian–Crimean–Caucasian region. M. Rakús, J. Dercourt, A. E. M. Nairn (Eds.), Evol. North. margin Tethys results IGCP Proj. 198, 154 (II), 103–124 , Paris: Mémoires de la Société Géologique.

Lyngsie, S.B., Thybo, H., Rasmussen, T.M., 2006, Regional geological and tectonic structures of the North Sea area from potential field modelling. Tectonophysics 413, 147–170.

Macpherson, C. G., Hall, R. 2001. Tectonic setting of Eocene boninite magmatism in the Izu-Bonin-Mariana forearc. Earth and Planetary Science Letters, 186. 215-230. http://dx.doi.org/10.1016/S0012-821X(01)00248-5

Mangino, S., Preistley, K., 1998. The crustal structure of the South Caspian region. Geophys. J. Int. 133, 630–648.

Maus, S. 2008. The geomagnetic power spectrum. Geophys. J. Int., 174, 135–142, doi:10.1111/j.1365-246X.2008.03820.x.

Maus, S., Barckhausen, U., Berkenbosch, H., et al., 2009. EMAG2: A 2-arc min resolution Earth Magnetic Anomaly Grid compiled from satellite, airborne and marine magnetic measurements. Geochemistry, Geophysics, Geosystems, 10, 1–24. https://doi.org/ 10.1029/2009gc002471

Maus, S., Gordon, D., Fairhead, D., 1997. Curie-temperature depth estimation using a self-similar magnetization model. Geophys. J. Int. 129, 163–168. https://doi.org/10.1111/ j.1365-246x.1997.tb00945.x

McNab, F., Ball, P. W., Hoggard, M. J., White, N. J. 2018. Neogene uplift and magmatism of Anatolia: Insights from drainage analysis and basaltic geochemistry. Geochemistry, Geophysics, Geosystems, 19, 175–213. https://doi.org/10.1002/ 2017GC007251

Mederer, J., Moritz, R., Ulianov, A., Chiaradia, M., 2013. Middle Jurassic to Cenozoic evolution of arc magmatism during Neotethys subduction and arc-continent collision in

the Kapan Zone, southern Armenia. Lithos 177, 61–78. https://doi.org/10.1016/j.lithos.2013.06.005

Mellors, R.J., Jackson, J., Myers, S., et al., 2012. Deep earthquakes beneath the northern Caucasus: Evidence of active or recent subduction in Western Asia. Bull. Seismol. Soc. Am. 102, 862–866. https://doi.org/10.1785/0120110184

Meyer, J., Hufen, J. H., Siebert, M., Hahn, A., 1985. On the identification of MAGSAT anomaly charts as crustal part of internal field. J. Geophys. Res., 90, 2537–2542.

Moghadam, H.S., Stern, R.J., 2015. Ophiolites of Iran: Keys to understanding the tectonic evolution of SW Asia: (II) Mesozoic ophiolites. Journal of Asian Earth Sciences, 100, 31-59. doi: http://dx.doi.org/10.1016/j.jseaes.2014.12.016

Moix, P., Beccaletto, L., Kozur, H.W., et al., 2008. A new classification of the Turkish terranes and sutures and its implication for the paleotectonic history of the region. Tectonophysics 451, 7–39. https://doi.org/10.1016/j.tecto.2007.11.044

Morris, A., 1996. A review of palaeomagnetic research in the Troodos ophiolite, Cyprus. Geol. Soc. London, Spec. Publ. 105, 311–324. https://doi.org/10.1144/GSL.SP.1996.105.01.27

Mosar, J., Kangarli, T., Bochud, M., et al., 2010. Cenozoic-Recent tectonics and uplift in the Greater Caucasus: A perspective from Azerbaijan. Geol. Soc. Spec. Publ. 340, 261–280. https://doi.org/10.1144/SP340.12

Mumladze, T., Forte, A.M., Cowgill, E.S., et al., 2015. Subducted, detached, and torn slabs beneath the Greater Caucasus. GeoResJ 5, 36–46. https://doi.org/10.1016/j.grj.2014.09.004

Mutlu, A. K., Karabulut, H. 2011. Anisotropic Pn tomography of Turkey and adjacent regions. Geophysical Journal International, 187, 1743–1758

Nairn, S.P., Robertson, A.H.F., Ünlügenç, U.C., Tasli, K., İnan, N., 2013. Tectono-stratigraphic evolution of the Upper Cretaceous–Cenozoic central Anatolian basins: an integrated study of diachronous ocean basin closure and continental collision. Geol. Soc. London, Spec. Publ. 372, 343–384. https://doi.org/10.1144/SP372.9

Neprochnov, Yu.P., Malovitsky, Ya.P., Belokurov, V.S., Garkalenko, I.A., 1975. Profile sections of the crust based on DSS. In: Boulanger, Yu.D. (Ed.), The Earth's crust and the history of the Black Sea evolution. Nauka, Moscow, 284–289 (in Russian).

Nikishin, A.M., Okay, A., Tüysüz, O., et al., 2015a. The Black Sea basins structure and history: New model based on new deep penetration regional seismic data. Part 2: Tectonic history and paleogeography. Mar. Pet. Geol. 59, 656–670. https://doi.org/10.1016/j.marpetgeo.2014.08.018

Nikishin, A.M., Okay, A.I., Tüysüz, O., et al., 2015b. The Black Sea basins structure and history: New model based on new deep penetration regional seismic data. Part 1: Basins structure and fill. Mar. Pet. Geol. 59, 638–655. https://doi.org/10.1016/j.marpetgeo.2014.08.017

Okay, A.I., Nikishin, A.M., 2015. Tectonic evolution of the southern margin of Laurasia in the Black Sea region. Int. Geol. Rev. 57, 1051–1076. https://doi.org/10.1080/00206814.2015.1010609

Okay, A.I., Tansel, İ., Tüysüz, O., 2001. Obduction, subduction and collision as reflected in the Upper Cretaceous–Lower Eocene sedimentary record of western Turkey. Geol. Mag. 138, 117–142. https://doi.org/10.1017/S0016756801005088

Okay, A.I., Tüysüz, O., 1999. Tethyan sutures of northern Turkey. Geol. Soc. London, Spec. Publ. 156, 475–515. https://doi.org/10.1144/GSL.SP.1999.156.01.22

Oufi, O., Cannat, M., Horen, H., 2002. Magnetic properties of variably serpentinized abyssal peridotites. J. Geophys. Res., 107(B5). https://doi.org/ 10.1029/2001JB000549.

Pearce, J., Bender, J., De Long, S., et al. 1990. Genesis of collision volcanism in eastern Anatolia, Turkey. Journal of Volcanology and Geothermal Research, 44(1-2), 189–229. https://doi.org/10.1016/0377-0273(90)90018-B

Pearce, J.A., Peate, D.W., 1995. Tectonic Implications of the Composition of Volcanic ARC Magmas. Annu. Rev. Earth Planet. Sci. 23, 251–285. https://doi.org/10.1146/ annurev.ea.23.050195.001343

Piromallo, C., Morelli, A., 2003. P wave tomography of the mantle under the Alpine-Mediterranean area. J. Geophys. Res. 108, 1–23. https://doi.org/10.1029/ 2002jb001757

Portner, D. E., Delph, J., Biryol, C. B., et al. (2018). Subduction termination through progressive slab deformation across Eastern Mediterranean subduction zones from updated P-wave tomography beneath Anatolia. Geosphere, 14, 907–925. https://doi.org/10.1130/GES01617.1

Robertson, A.H.F., Dixon, J.E., 1984. Introduction: aspects of the geological evolution of the Eastern Mediterranean. Geol. Soc. London, Spec. Publ. 17, 1–74. https://doi.org/ 10.1144/GSL.SP.1984.017.01.02

Robertson, A.H.F., Parlak, O., Ustaömer, T., 2009. Erratum to Melange genesis and ophiolite emplacement related to subduction of the northern margin of the Tauride–Anatolide continent, central and western Turkey. Geol. Soc. London, Spec. Publ. 311, 361–361. https://doi.org/10.1144/SP311.Erratum

Robertson, A.H.F., Parlak, O., Ustaömer, T., 2013. Late palaeozoic-early cenozoic tectonic development of southern Turkey and the easternmost Mediterranean region: Evidence from the inter-relations of continental and oceanic units. Geol. Soc. Spec. Publ. 372, 9–48. https://doi.org/10.1144/SP372.22

Rolland, Y., Galoyan, G., Sosson, M. et al., 2010. The Armenian Ophiolite: Insights for Jurassic back-arc formation, Lower Cretaceous hot spot magmatism, and Upper Cretaceous obduction over the South Armenian Block. Geol. Soc. London, Spec. Publ., 340, 353–382.

Ross, H.E., Blakely, R.J., Zoback, M.D., 2006. Testing the use of aeromagnetic data for the determination of Curie depth in California. GEOPHYSICS 71, L51--L59. https://doi.org/10.1190/1.2335572

Salaun, G., Pedersen, H. A., Paul, A., et al., 2012. High-resolution surface wave tomography beneath the Aegean-Anatolia region: constraints on upper-mantle structure. Geophysical Journal International, 190(1), 406–420. https://doi.org/ 10.1111/ j.1365-246X.2012.05483.x

Sandrin, A., Thybo, H., 2008. Seismic constraints on a large mafic intrusion with implications for the subsidence history of the Danish Basin. J. Geophys. Res. Solid Earth 113, 1–19. https://doi.org/10.1029/2007JB005067

Schaeffer, A.J., Lebedev, S., 2013. Global shear speed structure of the upper mantle and transition zone. Geophys. J. Int. 194, 417–449. https://doi.org/10.1093/gji/ggt095

Schildgen, T. F., Yıldırım, C., Cosentino, D., Strecker, M. R. 2014. Linking slab break-off, Hellenic trench retreat, and uplift of the Central and Eastern Anatolian Plateaux. Earth-Science Reviews, 128, 147–168.

Şengör, A.M.C., Lom, N., Sunal, G., Zabcı, C., Sancar, T., 2019. The phanerozoic palaeotectonics of Turkey. Part I: an inventory. Mediterr. Geosci. Rev. 1, 91–161. https://doi.org/10.1007/s42990-019-00007-3

Şengör, A.M.C., Natal'in, B.A., 1996. Paleotectonics of Asia: Fragments of a synthesis, in The Tectonic Evolution of Asia, edited by Y. An and T. M. Harrison, pp. 486–640,. Cambridge Univ. Press. Cambridge. 486–640.

Şengör, A.M.C., Yilmaz, Y., 1981. Tethyan evolution of Turkey: A plate tectonic approach. Tectonophysics 75, 181–241.

Şengör, A.M.C., Yilmaz, Y., Sungurlu, O., 1984. Tectonics of the Mediterranean Cimmerides: nature and evolution of the western termination of Palaeo-Tethys. Geol. Soc. London, Spec. Publ. https://doi.org/10.1144/GSL.SP.1984.017.01.04

Shapiro, N.M., Ritzwoller, M.H., 2004. Inferring surface heat flux distributions guided by a global seismic model: Particular application to Antarctica. Earth Planet. Sci. Lett. 223, 213–224. https://doi.org/10.1016/j.epsl.2004.04.011

Shive, P.N. et al., 1992. Magnetic properties of the lower crust. In: Fountain D.M., Arculus R., Kay R.W. (Eds.),Continental Lower Crust, Developments in Geotectonics, v. 23 Elsevier, New York, 145-178.

Siyako, M., Huvaz, O., 2007. Eocene stratigraphic evolution of the Thrace Basin, Turkey. Sediment. Geol. 198, 75–91. https://doi.org/10.1016/j.sedgeo.2006.11.008

Skolbeltsyn, G., Mellors, R., Gök, R., et al., 2014. Upper mantle S wave velocity structure of the East Anatolian-Caucasus region. Tectonics 33, 207–221. https://doi.org/10.1002/2013TC003334

Sosson, M., Rolland, Y., Müller, C., et al., 2010. Subductions, obduction and collision in the Lesser Caucasus (Armenia, Azerbaijan, Georgia), new insights. Geol. Soc. Spec. Publ. 340, 329–352. https://doi.org/10.1144/SP340.14

Sosson, M., Stephenson, R., Sheremet, Y., et al., 2016. The eastern Black Sea-Caucasus region during the Cretaceous: New evidence to constrain its tectonic evolution. Comptes Rendus Geosci. 348, 23–32. https://doi.org/10.1016/ j.crte.2015.11.002

Spector, A., Grant, G.S., 1970. Statistical Models for Interpreting Aeromagnetic data. Geophysics, 35, 293–302.

Stampfli, G.M., 2000. Tethyan oceans. Geol. Soc. London, Spec. Publ. 173, 1–23. https://doi.org/10.1144/GSL.SP.2000.173.01.01

Stampfli, G.M., 2000. Tethyan oceans. In: Bozkurt, E., Winchester, J.A., Piper, J.D.A. (Eds.), Tectonics and magmatism in Turkey and surrounding area. Geological Society of London Special Publication, 173, 1–23.

Stampfli, G.M., Borel, G.D., 2002. A plate tectonic model for the Paleozoic and Mesozoic constrained by dynamic plate boundaries and restored synthetic oceanic isochrons. Earth Planet. Sci. Lett. 196, 17–33. https://doi.org/10.1016/S0012-821X(01)00588-X

Stampfli, G.M., Borel, G.D., Cavazza, W., Mosar, J., Ziegler, P.A., 2001. Palaeotectonic and palaeogeographic evolution of the western Tethys and PeriTethyan domain (IGCP Project 369). Episodes 24, 222–228. https://doi.org/10.18814/epiiugs/2001/v24i4/001

Stern, R.J., Johnson, P., 2010. Continental lithosphere of the Arabian Plate: A geologic, petrologic, and geophysical synthesis. Earth-Science Rev. 101, 29–67. https://doi.org/10.1016/j.earscirev.2010.01.002

Talwani, M., Kessinger, W., 2003. Exploration Geophysics. In: R. A. Meyers (Ed.), Encyclopedia of Physical Science and Technology (3rd Edition), Academic Press, 709-726. https://doi.org/10.1016/B0-12-227410-5/00238-6.

Tatsumi, Y. and Eggins, S., 1995, Subduction Zone Magmatism. Blackwell, Oxford, 211 p Taymaz, T., Yilmaz, Y., Dilek, Y., 2007. The geodynamics of the Aegean and Anatolia: Introduction. Geol. Soc. Spec. Publ. 291, 1–16. https://doi.org/10.1144/SP291.1

Teknik, V., Ghods, A., 2017. Depth of magnetic basement in Iran based on fractal spectral analysis of aeromagnetic data. Geophys. J. Int. 209, 1878–1891. https://doi.org/10.1093/ gji/ggx132

Teknik, V., Ghods, A., Thybo, H., Artemieva, I.M., 2019. Crustal density structure of the northwestern Iranian Plateau. Can. J. Earth Sci. 56, 1347–1365. https://doi.org/10.1139/ cjes-2018-0232

Teknik, V., Thybo, H., Artemieva, I.M., Ghods, A., 2020. A new tectonic map of the Iranian plateau based on aeromagnetic identification of magmatic arcs and ophiolite belts. Tectonophysics. 792. https://doi.org/10.1016/j.tecto.2020.228588

Toft, P.B., Arkani-Hamed, J., Haggeryt, S.E., 1990. The effects of serpentinization on density and magnetic susceptibility: a petrophysical model. Physics of the Earth and Planetary Interiors, 65, 137-157.

Toksoz, M.N., Van der Hilst, R.D., Sun, Y., Zhang, H. 2008. seismic tomography of the Arabian-Eurasian collision zone and surrounding areas. Proc. 30th Monitoring Research Review: Ground-Based Nuclear Explosion Monitoring Technologies, Portsmouth, VA, v. 1, 504-513.

Topuz, G., Candan, O., Zack, T., Yilmaz, A. 2017. East Anatolian Plateau constructed over a continental basement: No evidence for the East Anatolian accretionary complex. Geology, 45(9). https://doi.org/10.1130/G39111.1

Topuz, G., Candan, O., Zack, T., Yilmaz, A., 2017. East Anatolian plateau constructed over a continental basement: No evidence for the East Anatolian accretionary complex. Geology 45, 791–794. https://doi.org/10.1130/G39111.1

Topuz, G., Okay, A.I., Altherr, R., Schwarz, W.H., Sunal, G., Altinkaynak, L., 2014. Triassic warm subduction in northeast Turkey: Evidence from the Ağvanis metamorphic rocks. Isl. Arc 23, 181–205. https://doi.org/10.1111/iar.12068

Turkoglu, E., Unsworth, M. J., Caglar, I., Tuncer, V., Avsar, U. 2008. Lithospheric structure of the Arabia-Eurasia collision zone in eastern Anatolia: Magnetotelluric evidence for widespread weakening by fluids? Geology, 36, 619–622.

Tutberidze, B., 2004. Geology and Petrology of Alpine Late Orogenic Magmatism of the Central Part of Caucasian Segment. Tbilisi University Publishers, Tbilisi, 1–340 (in Russian).

Taymaz, T., Yilmaz, Y., Dilek, Y., 2007. The geodynamics of the Aegean and Anatolia: Introduction. Geol. Soc. Spec. Publ. 291, 1–16. https://doi.org/10.1144/SP291.1

Vanacore, E. A., Taymaz, T., Saygin, E. 2013. Moho structure of the Anatolian Plate from receiver function analysis. Geophysical Journal International, 193, 329–337.

Varga, R.J., Karson J.A., Gee, J.S., 2004. Paleomagnetic constraints on deformation models for uppermost oceanic crust exposed in the Hess Deep Rift: Implications for axial processes at the East pacific Rise. J. Geophys. Res., 109, B0204. https://doi.org/10.1029/2003JB002486.

Vincent, S.J., Saintot, A., Mosar, J., Okay, A.I., Nikishin, A.M., 2018. Comment on "Relict Basin Closure and Crustal Shortening Budgets During Continental Collision: An Example From Caucasus Sediment Provenance" by Cowgill et al. (2016). Tectonics 37, 1006–1016. https://doi.org/10.1002/2017TC004515

Vinnik, L.P., Erduran, M., Oreshin, S.I., et al., 2014. Joint inversion of P- and S-receiver functions and dispersion curves of Rayleigh waves: The results for the Central Anatolian Plateau. Izv. Phys. Solid Earth 50, 622–631. https://doi.org/10.1134/S106935131404017X

Yegorova, T., Baranova, E., Murovskaya, A., et al., 2020. The crustal structure of the transition from the East Black Sea Basin to the Shatsky Ridge from reinterpretation of existing refraction seismic profiles 14-15-16. EAGG Proc., 2020, 1-5. https://doi.org/10.3997/2214-4609.2020geo021

Yılmaz, Y., Tüysüz, O., Yiğitbas, E., Genç, Ş.C., Şengör, A.M.C., 1997. Geology and tectonic evolution of the Pontides. In: A.G. Robinson (Ed.), Regional and Petroleum Geology of the Black Sea and Surrounding Region. AAPG Memoir 68, 183–226, Tulsa, OK.

Zakariadze, G.S., Dilek, Y., Adamia, S.A., et al., 2007. Geochemistry and geochronology of the Neoproterozoic Pan-African Transcaucasian Massif (Republic of Georgia) and implications for island arc evolution of the late Precambrian Arabian-Nubian Shield. Gondwana Res. 11, 92–108. https://doi.org/10.1016/j.gr.2006.05.012

Zanchi, A., Zanchetta, S., Berra, F., et al., 2009. The Eo-Cimmerian (Late? Triassic) orogeny in North Iran. Geol. Soc. London, Spec. Publ. 312, 31–55. https://doi.org/10.1144/SP312.3.

Zhou, S., Thybo, H. Power Spectra Analysis of Aeromagnetic Data and KTB Susceptibility Logs, and their Implication for Fractal Behavior of Crustal Magnetization. Pure appl. geophys. 151, 147–159 (1998). https://doi.org/10.1007/s000240050109.

Zonenshain, L.P., Pichon, X., 1986. Deep basins of the Black Sea and Caspian Sea as remnants of Mesozoic back-arc basins. Tectonophysics 123, 181–211. https://doi.org/10.1016/0040-1951(86)90197-6.

Zor, E. 2008. Tomographic evidence of slab detachment beneath eastern Turkey and Caucasus. Geophysical Journal International, 175, 1273–1282.

Figure captions

Figure 1: (a) Topography of Anatolia and adjacent regions based on ETOPO1 model (Amante and Eakins, 2009) with superimposed tectonic structures. Major tectonic units are separated by suture zones (after Okay and Tüysüz, 1999) associated with the closure of the Paleo-Tethys (Permian to Jurassic) and Neo-Tethys (Cretaceous–Cenozoic) oceans (thick white lines - major sutures (with question marks, where uncertain or debated), thin white lines -minor sutures; interpreted polarity of paleo-subduction zones is indicated by filled triangles). Black lines - major faults (after Taymaz et al., 2007): AF - Arax Fault, EAF - East Anatolian Fault, NAF - North Anatolian Fault, NTF - North Tabriz Fault.

(b) Major tectonic elements (after Okay and Tüysüz, 1999; Topuz et al., 2017; Şengör et al., 2019). Brown shading - on-shore magmatic zones (both felsic with weakly magnetized rocks and basaltic with iron-rich rocks, see **Figure 2**); black shading - ophiolites with iron-rich mafic and ultramafic rocks. The map is compiled from geological maps of Turkey (MTA, 2001, 1:1 250 000 Scale), Caucasus (2010, 1:1000 000 scale), Iran (2010, 1:1 00 000 scale), and Iraq (2012, 1:1 000 000 scale). Gray lines – coast lines and political boundaries. White lines as in (a). **Abbreviations:** TCFD -Terek Caspian foredeep, BMZ – Bitlis metamorphic zone.

Figure 2: (a) Typical maximum values of magnetic susceptibility in various rock types (based on compilation by Hunt et al., 1995. Vertical axis refers to both panels. Magenta line illustrates the general trend. **(b)** Empirical relationship between magnetic susceptibility and volume per cent of magnetite based on data reviewed by Toft et al. (1990). Black line for C=2.5 (Shive et al., 1992) marks the lower limit of data reviewed by Toft et al. (1990), who determined C=3.2 for ferromagnetic rocks. Black line labelled C=4.0 marks the upper limit of reported empirical values. **(c)** Curie temperature of titanomagnetites as function of the x-parameter (left) (Hunt et al., 1995); other magnetic minerals (middle); and young volcanoes in Cascadia, Variscan granites in Portugal, and rock examples from young oceanic crust (right) (Varga et al., 2004; Jackson and Bowles, 2014; Cruz et al., 2020). Vertical axis refers to all panels. **(d)** Effect of serpentinization of olivine plus pyroxene assemblages on magnetic susceptibility and density (based on data from Toft et al., 1990).

Figure 3: Possible relation between the seismically determined sediment thickness (depth to seismic basement, DSB), depth to magnetic basement (DMB), and the Curie depth point (CDP) below which iron-rich rocks lose their magnetization. **(a)** Lithosphere geotherm controls CDP. Cases 1-2: DSB can be deeper than DMB if the shallow part of the sedimentary cover hosts magnetized rocks, or if iron-rich rocks are all located below the CDP (e.g. in regions of active magmatism with a shallow CDP and with non-magnetic sediments). Cases 3-4: Depth to both seismic and magnetic basements are similar when magnetized mafic or ultramafic rocks lie immediately below the sedimentary cover. Cases 5-7: DSB is shallower than DMB when no magnetized iron-rich rocks are present within the sedimentary cover (e.g. when the sedimentary cover is thin or absent) but are present below sediments, and/or when lithosphere geotherm is cold so that mafic rocks of the lower crust preserve magnetization (case 7).

(b) Calculated profile of average crustal magnetic susceptibility (ACMS) (top panel) for various shapes of magnetic bodies buried at different depths under sedimentary rocks (bottom panel). Shallow highly magnetized bodies (e.g. basaltic intrusions) produce high-amplitude magnetic anomalies, usually with short wavelength variation, whereas deep-seated magnetized bodies produce low-amplitude, long-wavelength anomalies.

Figure 4: (a) Magnetic anomalies in Anatolia and neighboring regions. **(b)** The same with tectono-magmatic interpretation; magnetic anomalies are dimmed for clarity. The color scales are the same in (a) and (b). Triangles - Cenozoic volcanoes (http://www.volcano.si.edu/world). **See Table 1** for abbreviations. White lines as in **Figure 1a**.

Figure 5: (a) Depth to magnetic basement (DMB) from the topographic surface. Generally, the depth to magnetic basement inversely correlates with hypsometry and is larger in western Anatolia than in the high elevation regions of Eastern Anatolia and NW Iran.

(b) Thickness of sediments (Artemieva and Shulgin, 2019) compiled for the offshore domain from NOAA database updated for the Black Sea (Nikishin et al., 2015a) and for the on-shore domain based on the EUNAseis seismic model (Artemieva and Thybo, 2013) updated for Turkey (Gürbüz and Evans, 1991; Frederiksen et al., 2015) and the Arabian plate (Stern and Johnson, 2010). The thickness of sediments is not well constrained for many parts of the region due to a very limited number of seismic refraction and reflection profiles and borehole data. Color codes in (a) and (b) are the same. **See Table 1** for abbreviations. White lines as in **Figure 1a**.

Figure 6: (a) Difference between the seismically determined sediment thickness (DSB, **Figure 5b**) and depth to magnetic basement (DMB, **Figure 5a**). Warm colors (DSB>DMB) show regions with magnetized rocks (e.g. basalts, see **Figure 2**) in the shallow part of the sedimentary cover with possible outcrops (compare with **Figure 1b).** White color - regions with basalts or other magnetized rocks immediately below the sedimentary cover. Cold colors (DSB<DMB) indicate the presence of magnetized iron-rich rocks below the sedimentary cover. These regions are mostly in western Anatolia where scarce data suggests a thin sedimentary cover (i.e. small DSB values, case 6 in **Figure 3**), which together with a very shallow Curie depth point (<10-15 km) (Aydin et al., 2005; Artemieva and Shulgin, 2019) indicates that magnetized rocks are at shallow depth (with possible outcrops). For summary see **Table 2** and for explanations see **Figure 3**. White lines – suture zones, cf. **Figure 1**. This map should be interpreted with caution because the seismic thickness of sediments (depth to seismic basement) is poorly constrained in many parts of the region. **See Table 1** for abbreviations. **(b)** Curie depth in Anatolia (Aydin et al., 2005). **(c)** Statistical distribution of the [DSB - DMB] difference sampled on a 10 km × 10 km grid and plotted with 1 km bin size.

Figure 7: (a) Average crustal magnetic susceptibility (ACMS) with **(b)** superimposed magmatic outcrops (both felsic and mafic) and ophiolites. ACMS characterizes only magnetized crustal layers at temperatures below the Curie point. White lines – suture zones, cf. **Figure 1**. **See Table 1** for abbreviations.

Figure 8: (**a)** Gradient of average crustal magnetic susceptibility (ACMS). Black lines – outline of the most pronounced ACMS anomalies. ACMS heterogeneity increases from blue (relatively homogeneous values) to green (moderate heterogeneity) and to red, which corresponds to strongly heterogeneous regions with high-amplitude short-wavelength variations in ACMS. White lines - major suture zones; gray lines –coast and political boundaries.

(b) Characterization of crustal types based on integrated interpretation of susceptibility intensity (**Figure 7a**) and intensity gradient (**a**). H-magnetization (pink color) shows regions with high ACMS values and strong ACMS heterogeneity, interpreted as associated with magmatic arcs and voluminous basaltic magmatism. Several of these elongated magnetic anomalies (WKMA, NCMA, NBMA) have a similar NW-SE trend and NBMA appears to continue to the SE as

UDMA. PMA may extend to the west towards DMA. Numbers - paleosubduction dip angle estimated from widths of the magmatic arcs (**Figure 12**). Circular-shaped pink anomalies mark many of the basins. M-magnetization (green color) – regions with medium ACMS values and moderate heterogeneity. Hatched green-pink region in the south has characteristics in-between those corresponding to H- and M- anomalies. Its shape suggests that the Cyprus subduction system extends ca. 500 km eastwards into the N Arabian plate. L-magnetization (blue color) - regions with low, nearly uniform susceptibility, mostly in the southern (Gondwanian) part of the region. White lines - major suture zones; triangles show the polarity of paleosubduction systems; black lines –coast line and political boundaries. Dark blue and violet triangles show locations of Quaternary and Cretaceous volcanoes, respectively. **See Table 1** for abbreviations.

(c) Types of deep basins based on their magnetic susceptibility patterns, cf. **Table 4**. Pink color curves indicate H-magnetization areas (cf. **Figure 8b**) which may be associated with basaltic magmatism or trapped oceanic crust fragments in suture zones. The purple and red dashed lines show locations of the profiles in **Figures 10 and 11** with the width of the illustrated corridor marked by an **I** at the beginning of the lines.

Figure 9. Sketch illustrating the effects of crustal temperature and depth to magnetic bodies on amplitude and wavelength of variations in crustal magnetization for the same magnetic mineralogy. Amplitude (intensity) of crustal magnetization is shown in **Figure 7a**, wavelength of magnetization anomalies – in **Figure 8a**, depth – in **Figure 5a**, and a proxy to crustal temperatures – in **Figure 6b**.

Figure 10. Crust-mantle scale section along a NW-SE profile across some basins in Anatolia location shown in **Figure 8c**.

(a) Variation in average crustal magnetic susceptibility (ACMS); highlighted strong anomalies mainly occur above major known basins. Type of basin (cf. Table 4) is marked above the profile.

(b) Cross section of the uppermost crust showing the depth to magnetic basement. Sedimentary basins are highlighted with dark green and high ACMS is highlighted by pink area in the basement.

(c) Shear velocity model along the profile (from Kaviani et al., 2020), illustrating also depth to Moho. Black small circles show location of seismic events (http://www.isc.ac.uk/isc-ehb/search/catalogue).

Figure 11. Two SW-NE striking profiles (for location see **Figure 8c**; left: western profile, right: eastern profile) across Anatolia between the Mediterranean Sea and the Black Sea.

a,b: Averaged crustal magnetic susceptibility (ACMS) profiles, strong anomalies are highlighted in pink.

c,d: Depth to magnetic basement (DMB). Major sedimentary basins are highlighted by dark green, strong ACMS anomalies are highlighted by pink in the basement. Location of major sutures are marked (cf. **Figure 1).**

e,f: Crustal and uppermost mantle shear-wave velocity (Kaviani et al., 2020); dashed lines show Moho depth. Black small circles indicate location of seismic events (http://www.isc.ac.uk/isc-ehb/search/catalogue). The active Cyprus subduction (blue dashed line) and paleo-subductions (dark red lines) control the location of magmatic arcs.

g,h: P-wave velocity based on teleseismic tomography (Portner et al., 2018). Low velocity beneath WKMA may indicate the source of magmatic activity that led to strong ACMS. High velocity correlates with the Cyprus slab with a possible slab tearing which creates mantle flow that may amplify the intensity of magmatism beneath WKMA.

Figure 12. Correlation between subduction angle and magmatic arc width (blue circles and best-fit line based on Tatsumi and Eggins, 1995) allow for estimating dip angle of the Tethyan subduction systems (colored rectangles). The width of the vertical rectangles corresponds to the width of the inferred magmatic arcs and the horizontal rectangles indicate the range of estimated subduction angles for magmatic arcs in the study region, cf. abbreviations in figure legend.

Figure 1

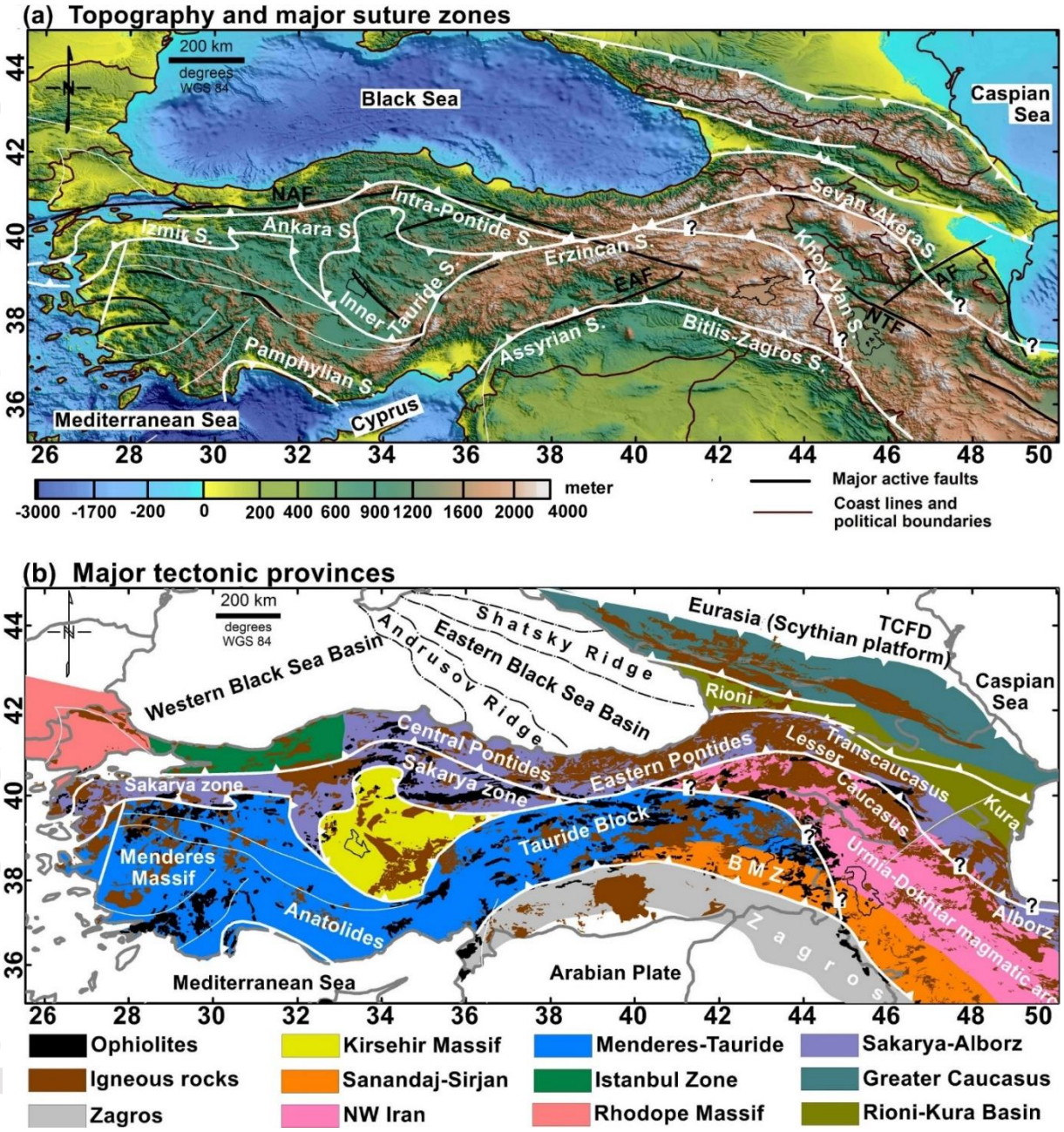

Figure 2

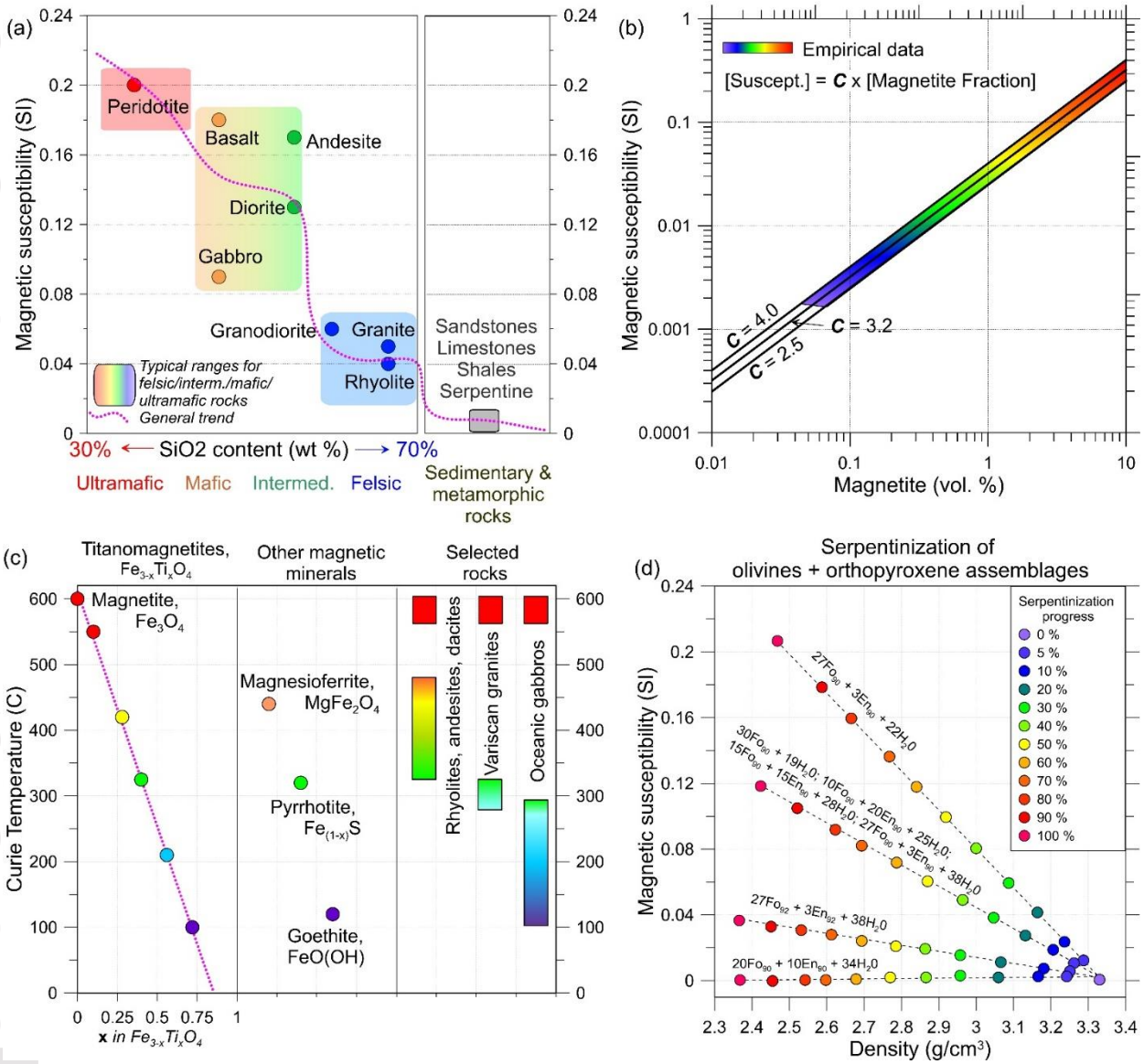

Figure 3

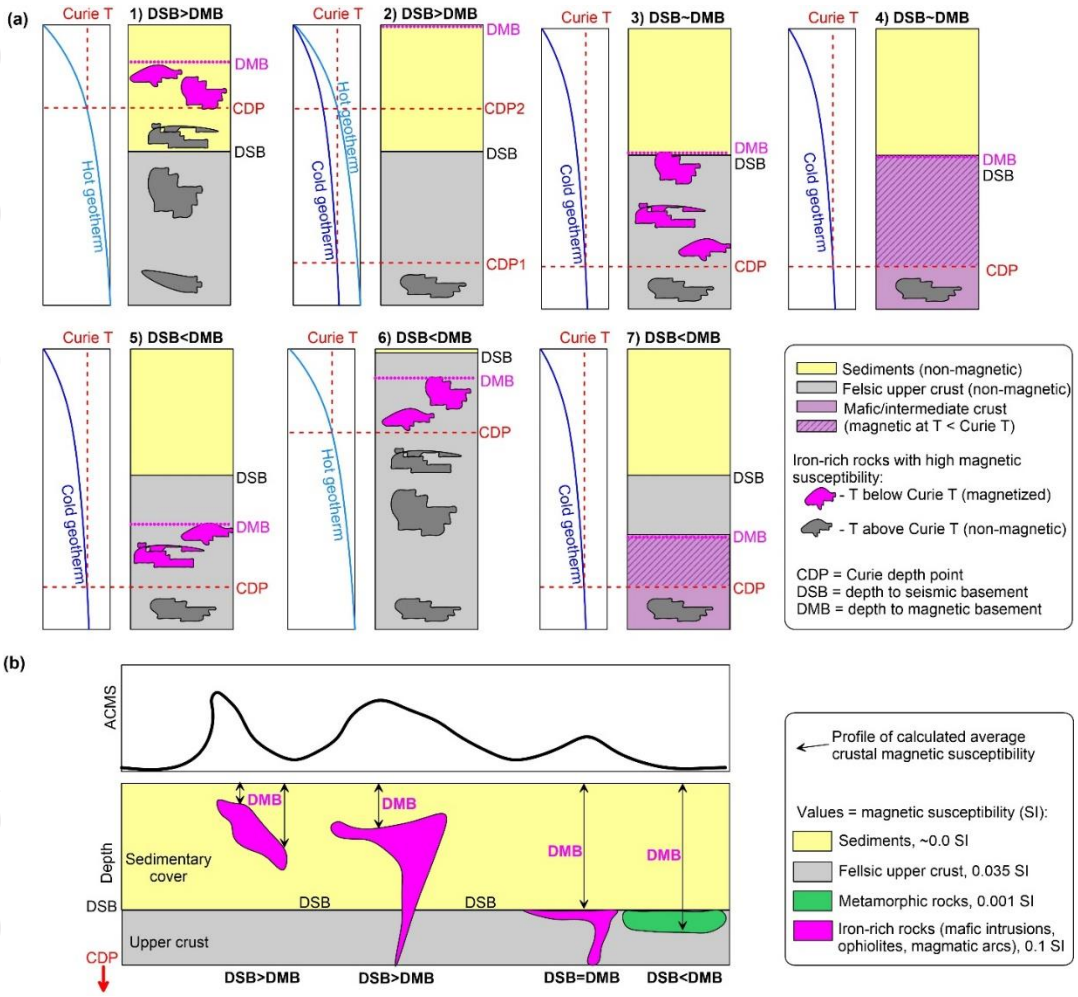

Figure 4

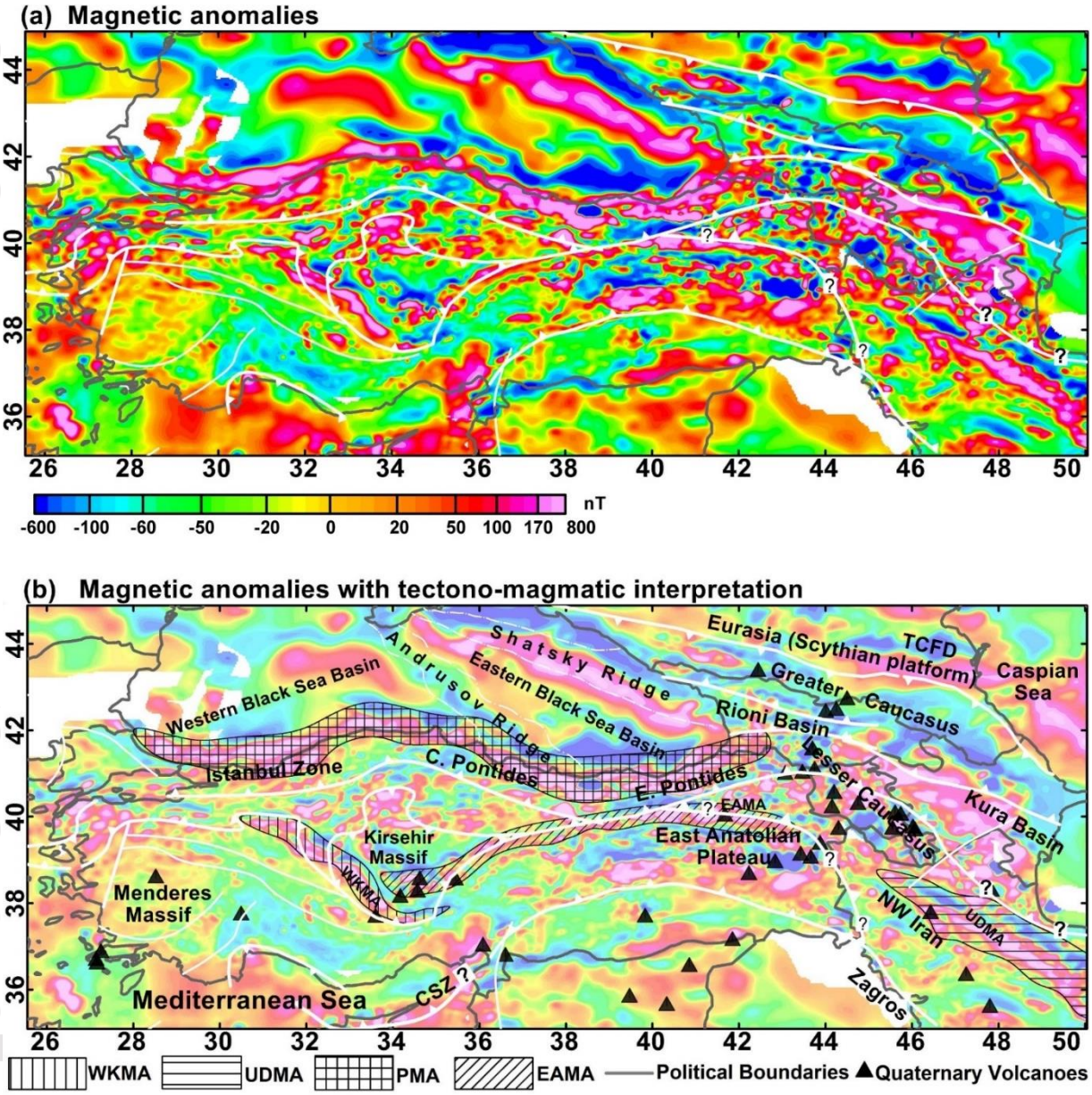

Figure 5

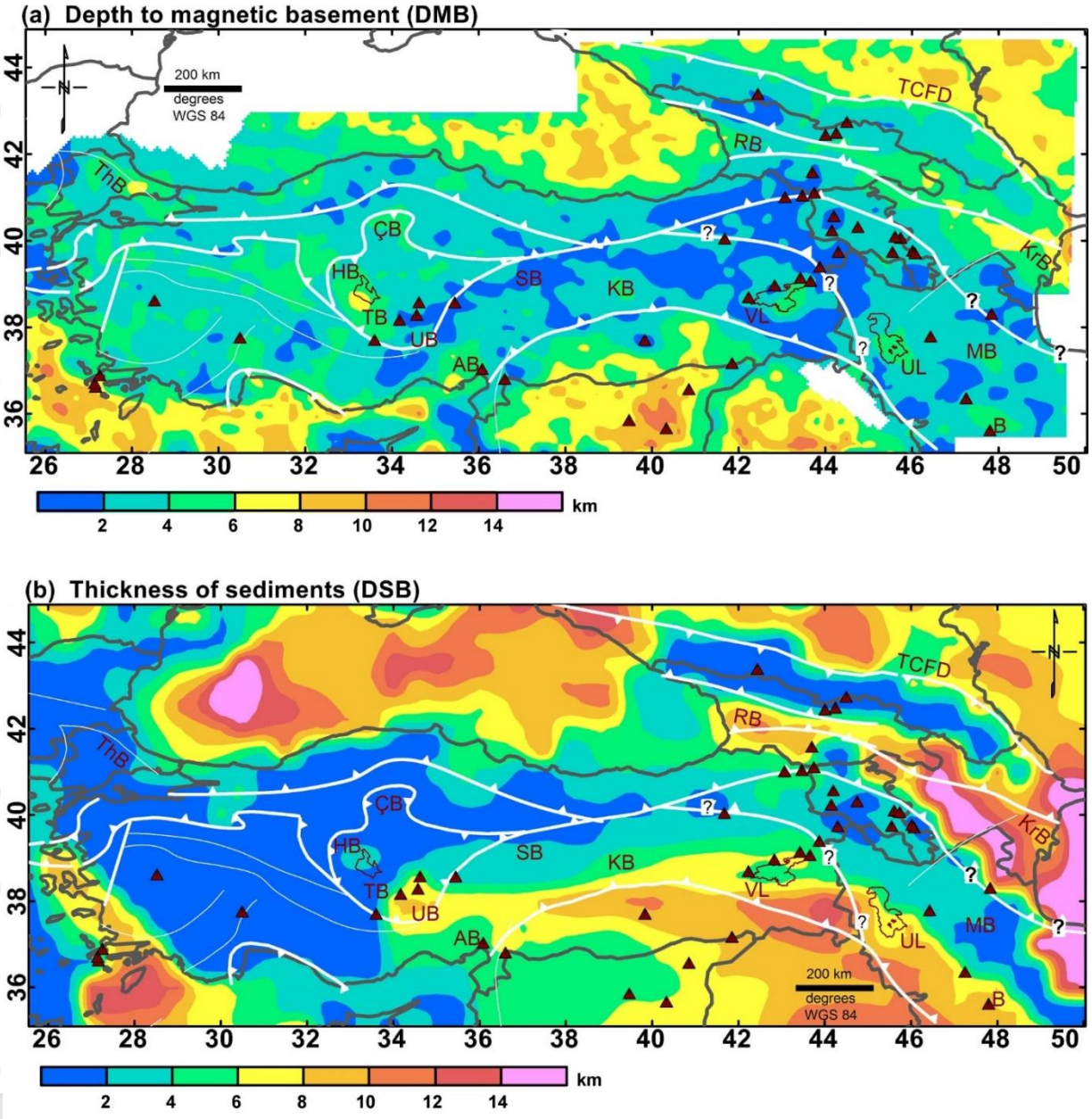

Figure 6

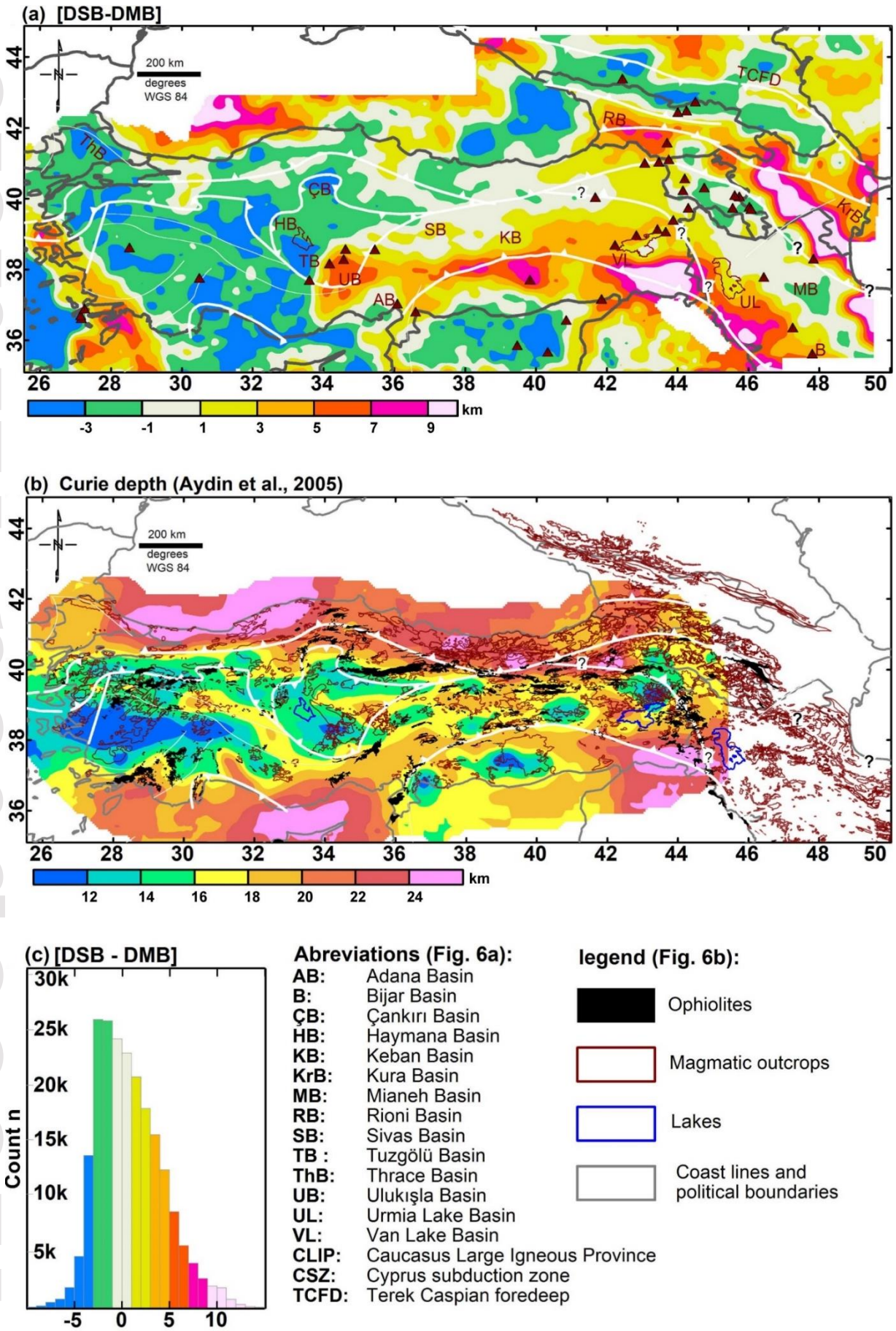

Figure 7

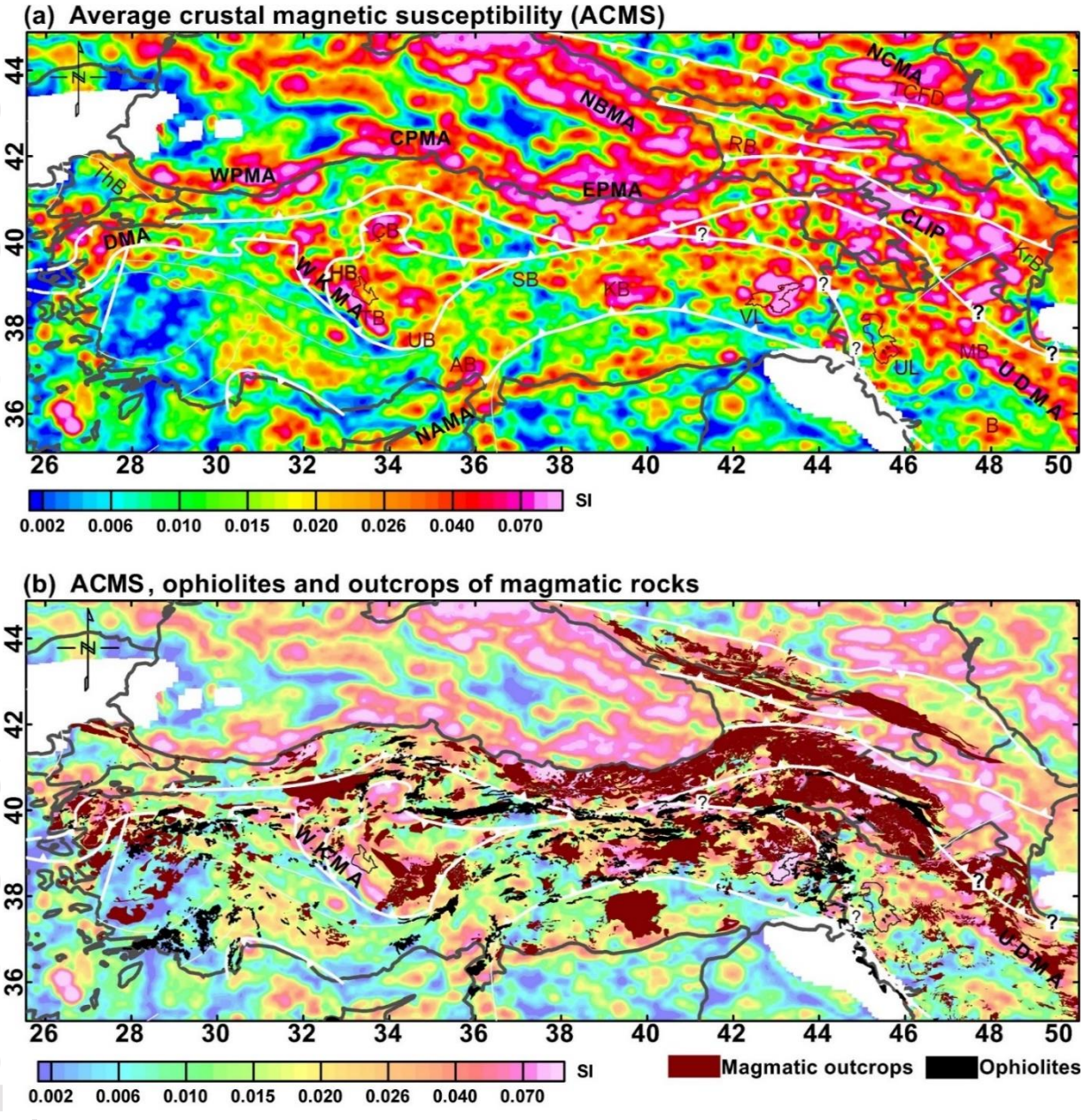

Figure 8

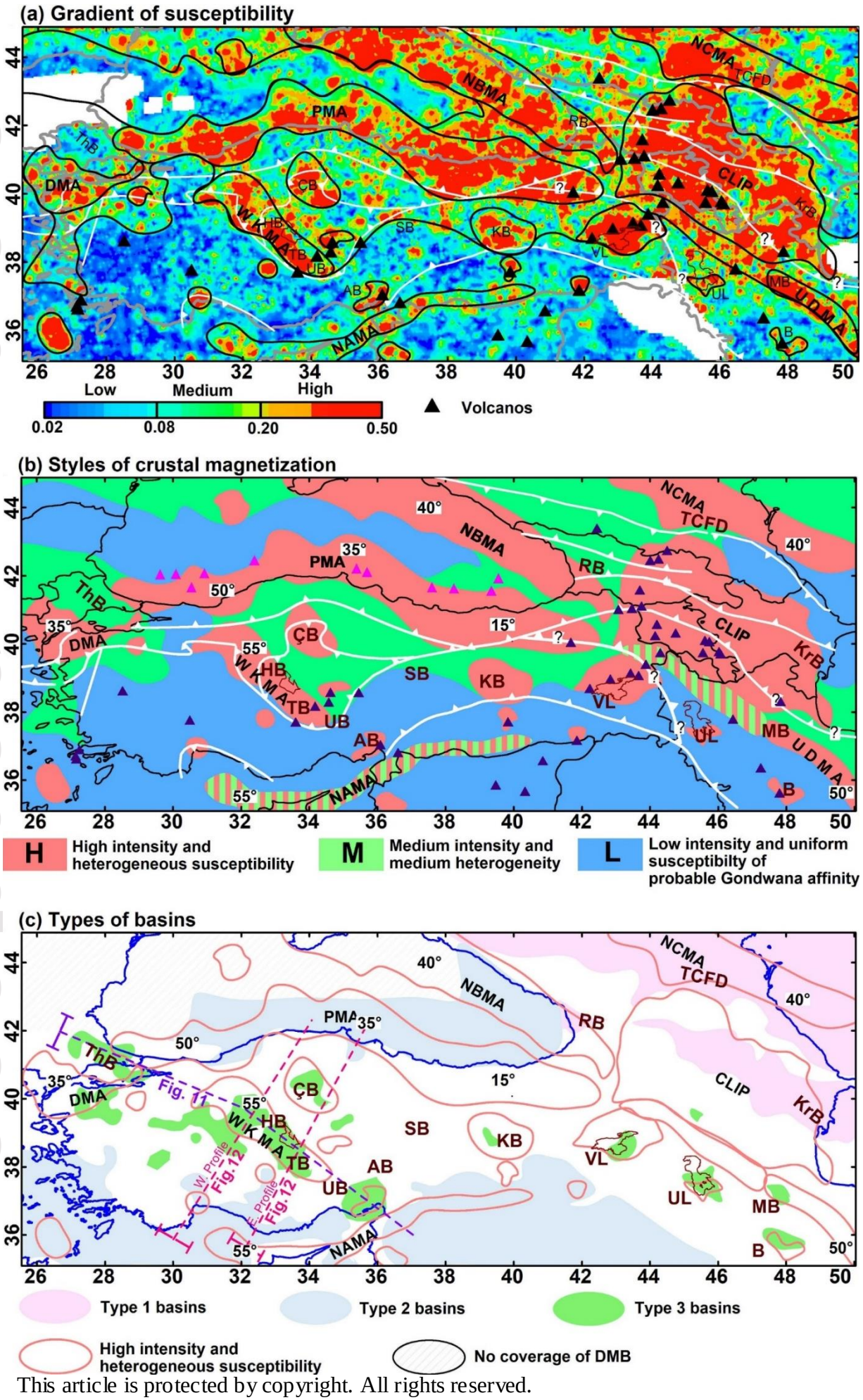

Figure 9

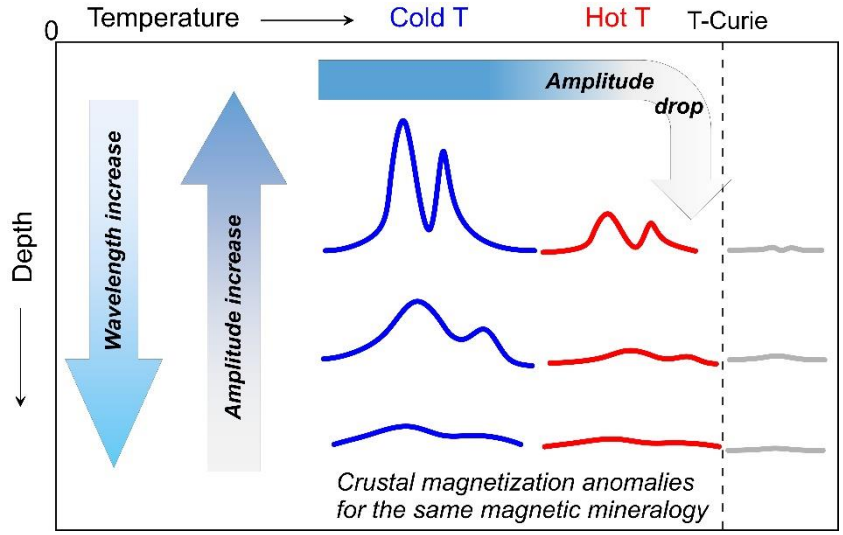

Figure 10

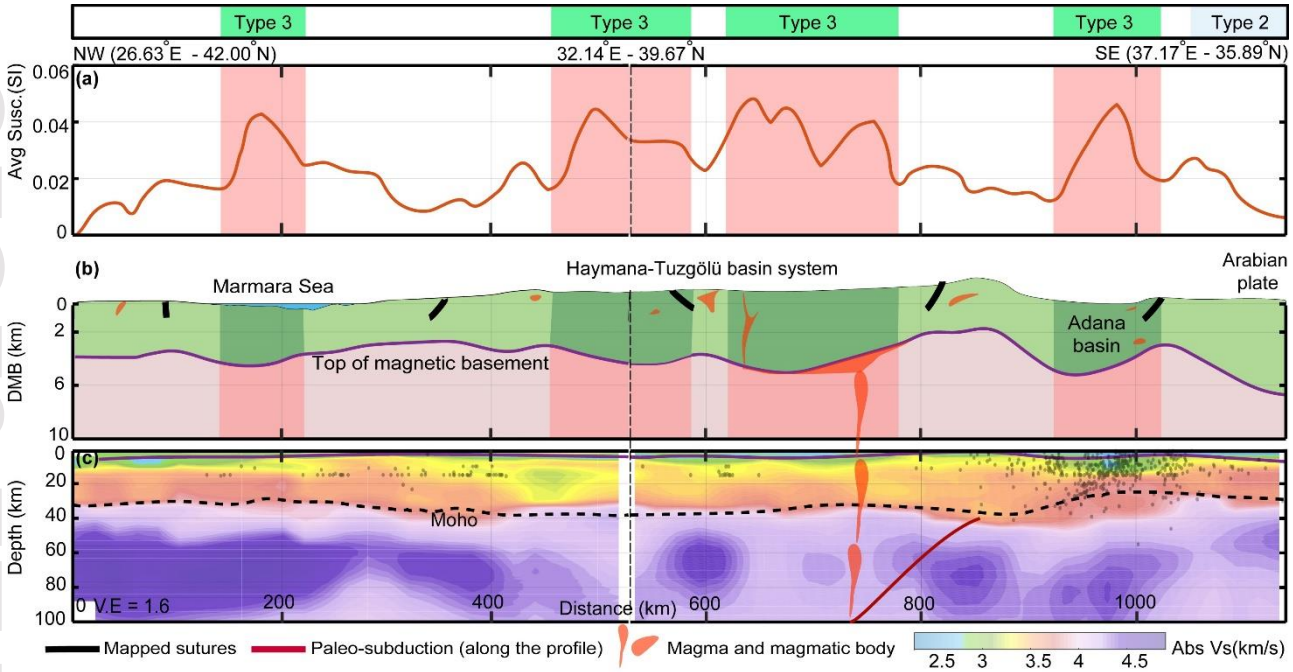

Figure 11

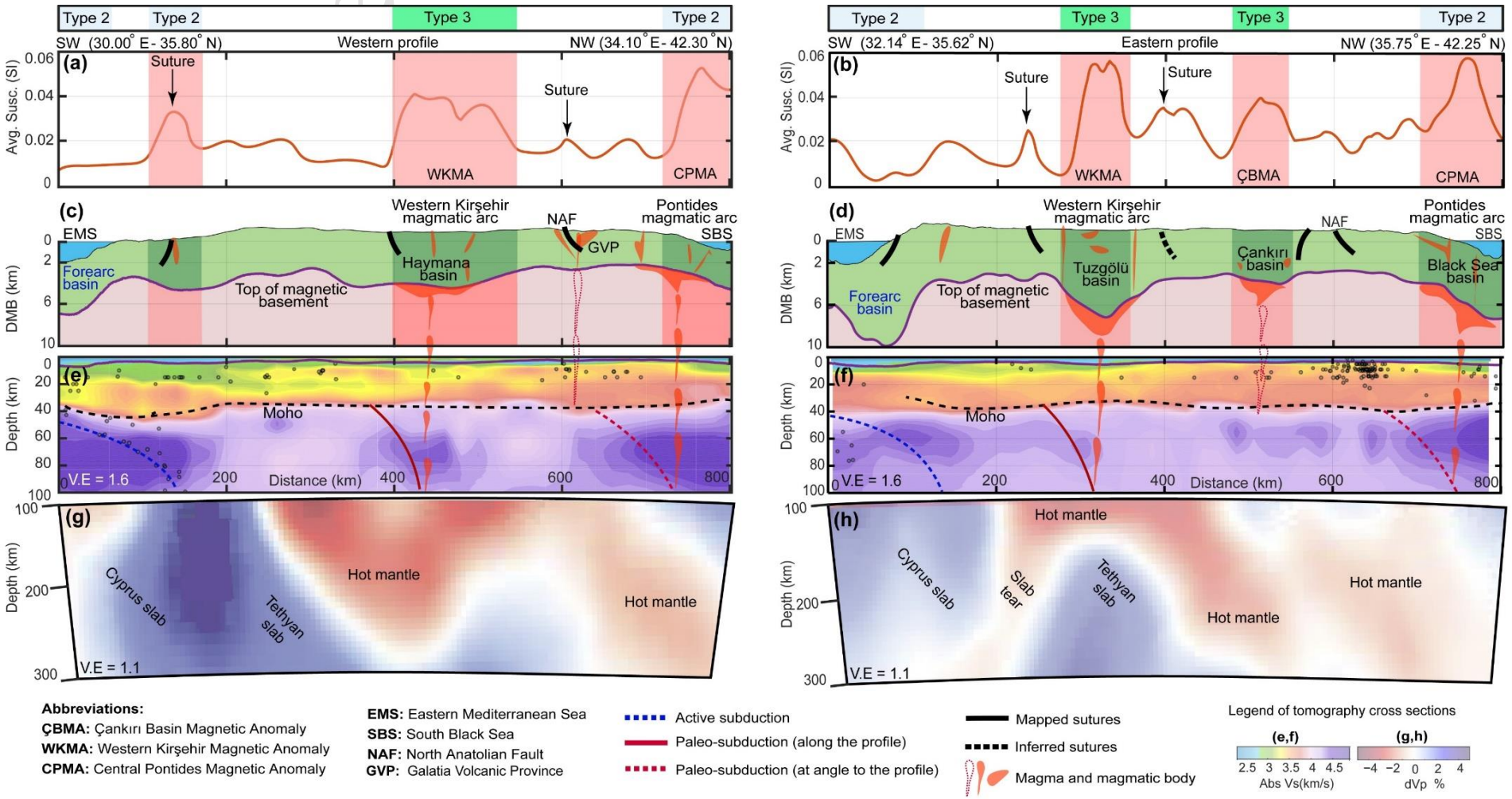

Figure 12

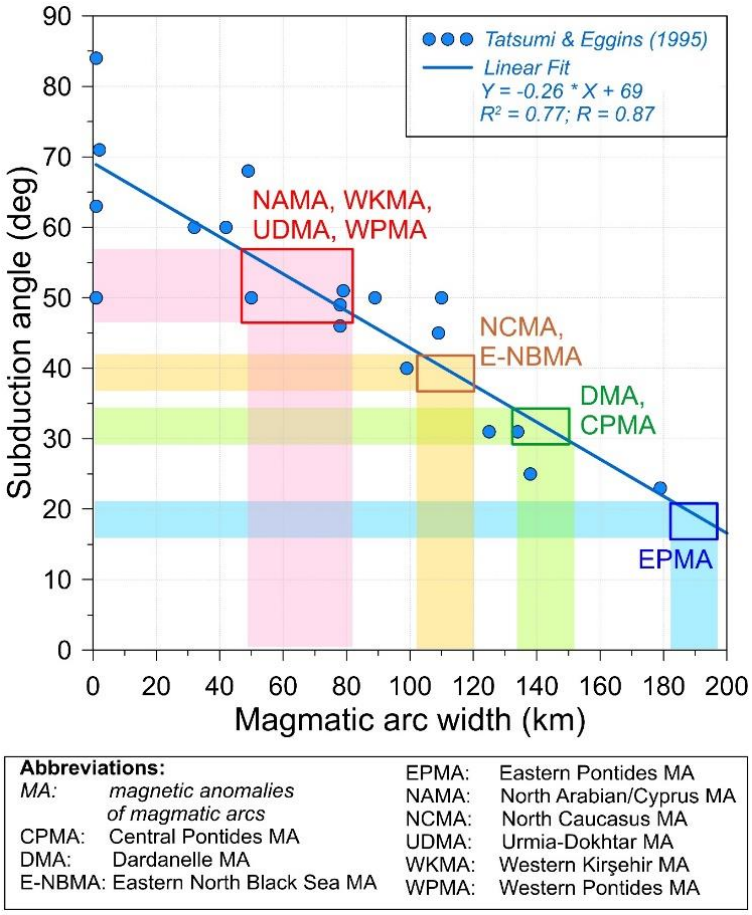

Abbreviations:

MA: *magnetic anomalies of magmatic arcs*
CPMA: Central Pontides MA
DMA: Dardanelle MA
E-NBMA: Eastern North Black Sea MA
EPMA: Eastern Pontides MA
NAMA: North Arabian/Cyprus MA
NCMA: North Caucasus MA
UDMA: Urmia-Dokhtar MA
WKMA: Western Kirşehir MA
WPMA: Western Pontides MA

The below mentioned reference is available in the reference section, however it is not cited in the text.

1. Adamia et al., 1981

Remove it

2. Clark and Emerson, 1991

Add to the 7th line of the first paragraph of the section of 3.2 Magnetic susceptibility. Update to (Clark and Emerson, 1991; Hunt et al., 1995)

3. Mangino and Preistley, 1998

Add to the line of 6 of the first paragraph of the sub section of "Rioni-Kura Basins in the Transcaucasus region" from section of "2.2. Major terranes and tectonic units". Update the citation to (cf. Mangino and Preistley, 1998, Krasnopevtseva, 1984; Artemieva and Thybo, 2013)

4. Nikishin et al., 2015b

All citation in the text from (Nikishin et al., 2015) to (Nikishin et al., 2015b)

5. Robertson et al., 2009

Add to line 6th of the first paragraph of the sub section of "Anatolides and Taurides" from section of "2.2. Major terranes and tectonic units". Update the citation to (Gürer et al., 2016; Robertson et al., 2009)

6. Teknik et al., 2019

Add to the 5th line of the first paragraph of the sub section of "Zagros orogen and NW Iran" from section of "2.2. Major terranes and tectonic units". Update the citation to (Moghadam and Stern, 2015; Teknik et al., 2019).

The below listed references are cited in the text, however the references are not provided in the reference section.

1. Cowgill et al., 2016
2. Stephensen and Schellart, 2010

Correct it to (Stephenson and Schellart, 2010)

3. Nikishin et al., 2015

Correct it to Nikishin et al., 2015b

4. Taymaz et al., 2007
5. Kaymakci et al., 2000

Correct it to (Kaymakçi, 2000)

6. Artemieva and Thybo, 2013

(Artemieva and Thybo, 2013). The reference is in the line of the 1259 in the main text

7. Dirik et al., 1999

(Dirik et al., 1999); The reference is exist in the line of the 1322 in the main text

References:

Artemieva, I.M., Thybo, H., 2013. EUNAseis: A seismic model for Moho and crustal structure in Europe, Greenland, and the North Atlantic region. Tectonophysics 609, 97–153. https://doi.org/10.1016/j.tecto.2013.08.004

Cowgill, E., Forte, A.M., Niemi, N., Avdeev, B., Tye, A., Trexler, C., Javakhishvili, Z., Elashvili, M., Godoladze, T., 2016. Relict basin closure and crustal shortening budgets during continental collision: An example from Caucasus sediment provenance. Tectonics 35, 2918–2947. https://doi.org/10.1002/2016TC004295

Dirik, K., Göncüoğlu, M.C., Kozlu, H., 1999. Stratigraphy and pre-Miocene tectonic evolution of the southwestern part of the Sivas Basin, Central Anatolia, Turkey. Geol. J. 34, 303–319. https://doi.org/10.1002/(SICI)1099-1034(199907/09)34:3<303::AID-GJ829>3.0.CO;2-Z

Kaymakçi, N., 2000. Tectono-stratigraphical evolution of the Çankırı Basin (Central Anatolia, Turkey). Geol. Ultraiectina.

Stephenson, R., Schellart, W.P., 2010. The Black Sea back-arc basin: insights to its origin from geodynamic models of modern analogues. Geol. Soc. London, Spec. Publ. 340, 11–21. https://doi.org/10.1144/SP340.2

Taymaz, T., Yilmaz, Y., Dilek, Y., 2007. The geodynamics of the Aegean and Anatolia: Introduction. Geol. Soc. Spec. Publ. 291, 1–16. https://doi.org/10.1144/SP291.1